

Interaction Notes

Note 182

July 1974

Impedances and Field Distributions of Two Coplanar Parallel  
Perfectly Conducting Strips with Arbitrary Widths

Tom K. Liu

The Dikewood Corporation, Westwood Research Branch  
Los Angeles, California 90024

Abstract

In this report, transmission lines in the form of two coplanar parallel conducting strips with arbitrary widths are studied. This kind of coplanar strip lines finds application in many aircraft antennas. The geometrical impedance factor, which relates the characteristic impedance of the transmission line to the intrinsic impedance of the medium surrounding the strips, is plotted and tabulated. The field distributions of the strips are also plotted. When compared to a two-cylinder transmission line with the radii of the cylinders being equal to the strip widths and the cylinders being separated by the same distance as the strips, the geometrical impedance factor of the strips is larger than that of the cylinders by approximately a constant  $(\ln 2)/\pi$ .

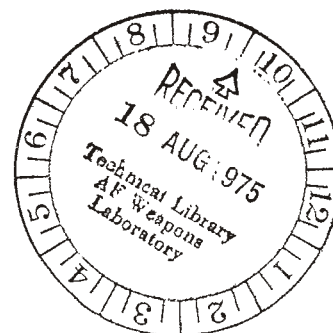


## Table of Contents

	Page
Abstract	1
Section	
I    Introduction	5
II   Mathematical Formulation and Results	7
III  Coplanar Strip Lines and Two-Cylinder Transmission Lines	30
IV   Other Configurations Related to that of the Present Problem	40
V    Conclusions	44
Acknowledgement	
References	

## Illustrations

### Figure

1	Cross-sectional view of the two coplanar strips of unequal widths.	6
2	(a) The $z$ -plane containing the two coplanar strips of unequal widths and, (b) The $z_1$ -plane containing the transformed coplanar strips of equal width.	8
3	(a) The $z_1$ -plane containing two strips of equal width and, (b) The $w$ -plane resulting from the Schwarz-Christoffel transformation.	11
4	The geometrical impedance factor versus $a/d$ with $b/d$ as a parameter. The case $a = b$ is also plotted. Note the change in abscissa scale.	15
5	Field distribution of the two coplanar strips. $a/d = 0.2$ , $b/d = 0.2$ .	20
6	Field distribution of the two coplanar strips. $a/d = 0.5$ , $b/d = 0.5$ .	21
7	Field distribution of the two coplanar strips, $a/d = 1$ , $b/d = 0.2$ .	22
8	Field distribution of the two coplanar strips, $a/d = 1$ , $b/d = 1$ .	23
9	Field distribution of the two coplanar strips, $a/d = 2$ , $b/d = 1$ .	24
10	Field distribution of the two coplanar strips, $a/d = 2$ , $b/d = 2$ .	25
11	Field distribution of the two coplanar strips, $a/d = 5$ , $b/d = 1$ .	26
12	Field distribution of the two coplanar strips, $a/d = 10$ , $b/d = 1$ .	27
13	Field distribution of the two coplanar strips, $a/d = 10$ , $b/d = 2$ .	28
14	Field distribution of the two coplanar strips, $a/d = 10$ , $b/d = 10$ .	29
15	The cross-sectional view of a two-cylinder transmission line.	31
16	A comparison of the strip transmission line with a two-cylinder transmission line.	32

Figure		
17	The geometrical impedance factor of a strip transmission line of equal strip width and of a two-cylinder line with the cylinder radii equal to one quarter of the strip width. The percentage difference of the two factors is shown as the dashed line.	34
18	A comparison of the strip transmission line with a two-cylinder transmission line.	36
19	The geometrical impedance factor of a strip transmission line of equal strip width and of a two-cylinder transmission line with radii equal to one half of the strip width. The percentage deviation of the difference of the two factors from $(\ln 2)/\pi$ is shown as the dashed line.	38
20	The percentage deviation of the difference of the two geometrical impedance factors (of the strip line and the two-cylinder line with radii being equal to one half of the strip widths) from $(\ln 2)/\pi$ .	39
21	(a) The coplanar strips configuration and its related configuration such as (b) one section of an infinite stack of parallel strips, (c) a strip between two infinite ground planes and (d) the conventional strip line.	41
22	The biconical transmission line and its stereographic projection - the coplanar strips.	42
23	Problems related to the coplanar strips by inversion (a) a strip inside a cylinder (b) a cylinder inside a slit (c) a strip inside a slot.	43
Table I	The geometrical impedance factor for $a/d \leq 0.1$ .	16
Table II	The geometrical impedance factor for $0.1 \leq a/d \leq 1$ .	17
Table III	The geometrical impedance factor for $1 \leq a/d \leq 10$ .	18
Table IV	The geometrical impedance for $a/d \geq 10$ .	19

## I. Introduction

In the course of analyzing deliberate aircraft antennas, transmission lines in the form of two coplanar parallel conducting strips with unequal widths have been encountered. Such transmission lines are used in the glide slope track antenna [1] and the VHF communication antenna no.1 [11], both being on an AABNCP; and also in the HF antenna on a B-1 [2]. Therefore, it is necessary to study this kind of transmission lines to obtain the characteristic impedances that are essential in the antenna analyses. In this report, two coplanar parallel strip conductors of arbitrary widths are studied, and the geometrical impedance factors and the field distributions of various configurations of the structure are presented in graphical and/or tabular form.

The configuration under study is shown in Fig.1, where the widths of the strips are  $a$  and  $b$ , and they are separated by a distance  $d$ . Since, in practice the thickness of the strips are small compared with the widths, we assume a zero thickness in our analysis. This greatly simplifies the analysis without sacrificing too much accuracy. Related problems have been studied by Baum [3], Carlisle [4] and Hayt [5]; the latter investigated the problem of three symmetrical staggered plates of finite widths (i.e., the conventional strip line) using conformal mapping techniques. In this report, the problem is solved by using conformal mappings different from those of Hayt and simpler expressions are obtained. Because of the popular usage of two-cylinder transmissions lines, we also make a comparison between the coplanar strips with the parallel cylinders.

In section II, the conformal mapping procedures are detailed and the expressions for the geometrical impedance factor and for the field distributions are presented. Numerical results of these two quantities are given in graphical and tabular forms for a few geometric configurations. The comparison between the coplanar strip line and the two-cylinder transmission line is presented in section III. Finally in section IV, we outline some possible extensions of the results in this report to other geometries.



Fig.1. Cross-sectional view of the two coplanar strips of unequal widths.

## II. Mathematical Formulation and Results

It is known that by using a Jacobian elliptic function transformation [6], two coplanar strips of equal width can be conformally mapped into a rectangle in the transformed plane from which the potential distribution is readily found. The first step in our analysis is to map the two strips of arbitrary widths into two strips of equal width, using a bilinear transformation.

The two coplanar strips are shown in the  $z$ -plane in Fig. 2a. One strip is at  $y = 0$  from  $x = -a$  to  $x = 0$  and the other is at  $y = 0$  from  $x = d$  to  $x = d + b$ . By symmetry of this structure, the remainders of the  $x$ -axis apart from the two strips are field lines, on which  $d\phi/dy = 0$  with  $\phi$  being the potential.

The bilinear transformation is of the following form:

$$z_1(z) = \frac{z+c_0}{c_1z+c_2} \quad (1)$$

where

$$z = x + iy, \quad (2)$$

$$z_1 = x_1 + iy_1. \quad (3)$$

The three values  $c_0$ ,  $c_1$  and  $c_2$  are determined by selecting the locations of three transformed points in the  $z_1$ -plane. In Fig. 2b, we choose point  $D$  in the  $z$ -plane to be mapped into point  $D_1$  in the  $z_1$ -plane such that

$$z|_D \rightarrow z_1|_{D_1} = -1.$$

Similarly,

$$z|_F \rightarrow z_1|_{F_1} = 1$$

and

$$z|_B \rightarrow z_1|_{B_1} \quad \text{and} \quad z|_G \rightarrow z_1|_{G_1}$$

such that

$$z_1|_{G_1} = -z_1|_{B_1} = h \quad (4)$$

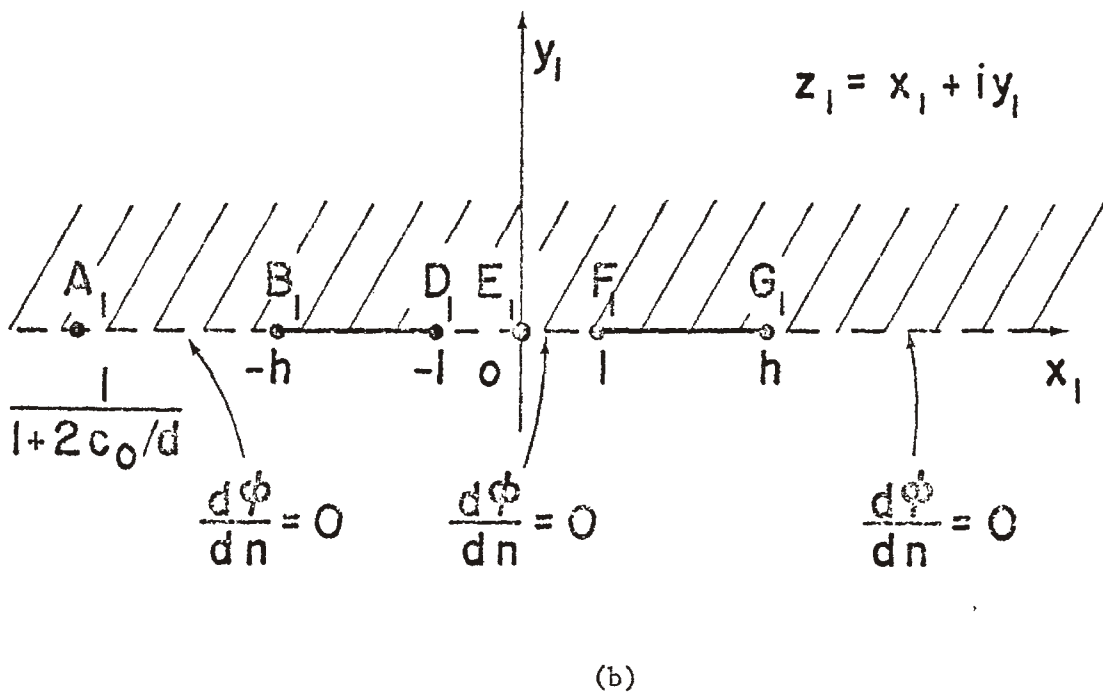
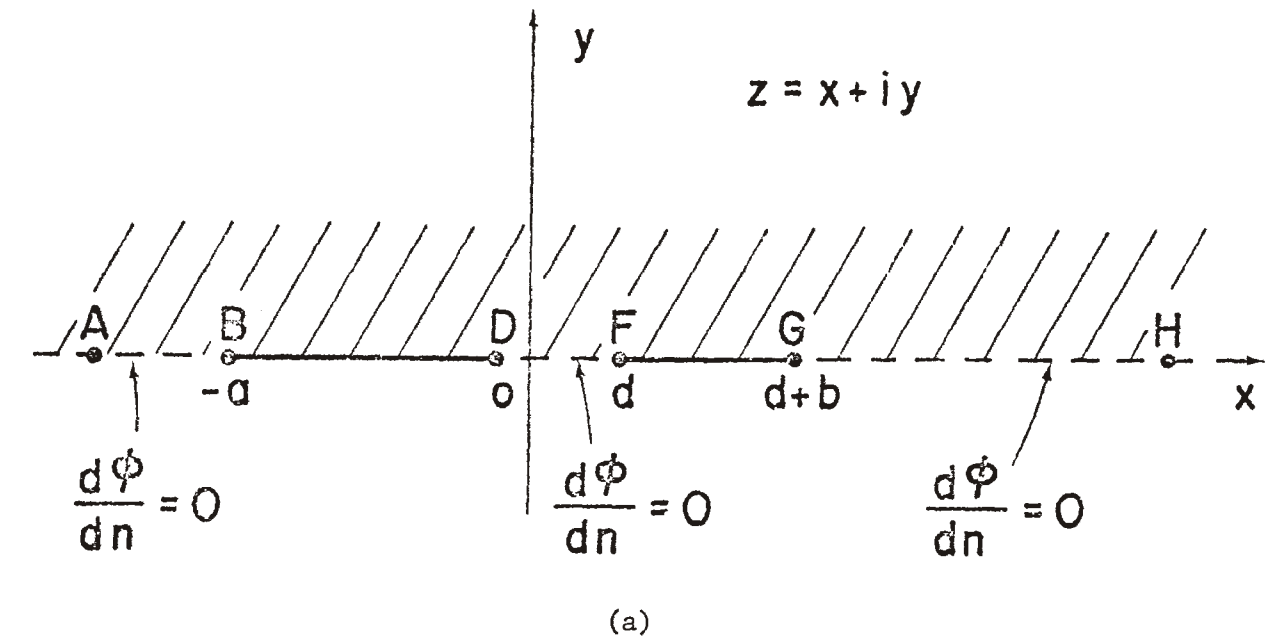


Fig.2. (a) The  $z$ -plane containing the two coplanar strips of unequal widths and,  
 (b) The  $z_1$ -plane containing the transformed coplanar strips of equal width.



where  $h$  is a positive real number. The transformation now becomes

$$z_1(z) = \frac{z+c_0}{(1+2c_0/d)z-c_0} \quad (5)$$

where

$$c_0 = \{-a(b+d) \pm [ab(a+d)(b+d)]^{1/2}\} / (a-b) \quad \text{for } a \neq b \quad (6a)$$

$$= -d/2 \quad \text{for } a = b \quad (6b)$$

The infinity points  $A$  and  $H$  in the  $z$ -plane are now transformed into point  $A_1$ , where

$$z_1|_{A_1} = (1 + 2c_0/d)^{-1} \quad (7)$$

and, in the symmetrical case  $a = b$ ,

$$z_1|_{A_1} \rightarrow \infty$$

The mapping of Fig. 2b into a rectangle can be achieved by means of a Schwarz-Christoffel transformation. It can be shown that the mapping is of the following form:

$$w(z_1) = P \int_0^{z_1} [(1-\lambda^2)(1-m\lambda^2)]^{-1/2} d\lambda + Q \quad (8)$$

where

$$m = 1/h^2 = 1/[z_1(-a)]^2 \quad (9)$$

and  $P$  and  $Q$  are constants to be determined. The integral in (8) is an inverse Jacobian elliptic function [7] and (8) can be re-written as

$$w(z_1) = P \operatorname{sn}^{-1}(z_1|m) + Q \quad (10)$$

We first choose the plus sign (in the sign of ambiguity) in (6a). It can be readily shown that this selection results in a value of  $m$ , as defined

in (9), such that

$$0 \leq m \leq 1 \quad (11)$$

This is the range of  $m$  values within which values of the elliptic functions are available [7]. We then select the transformed location of  $A_1$  (i.e. the infinity of the  $z$ -plane) such that the potential there is zero. Physically, this means that we define the potential at infinity of the original problem to be zero. This automatically imposes the condition that the total charges on the two strips are equal but opposite. This condition ensures the problem to be a well-defined one. We select the following transformation conditions (see Fig. 3)

$$z_1|_{D_1} \rightarrow w|_{D_2} = -u_0 \quad (12a)$$

$$z_1|_{F_1} \rightarrow w|_{F_2} = 2 - u_0 \quad (12b)$$

$$z_1|_{G_1} \rightarrow w|_{G_2} = 2 - u_0 + iv_0 \quad (12c)$$

$$z_1|_{A_1} \rightarrow w|_{A_2} = 0 + iv_1 \quad (12d)$$

These conditions are chosen so that the equipotential lines are at  $u = \text{constant}$  inside the rectangle. The resulting mapping is in Fig. 3b. The first three conditions in (12) yield the following values:

$$P = 1/K(m),$$

$$v_0 = K(m_1)/K(m) \quad (13)$$

and

$$Q = 1 - u_0 \quad (14)$$

where  $K(m)$  is the complete elliptic function of the first kind and

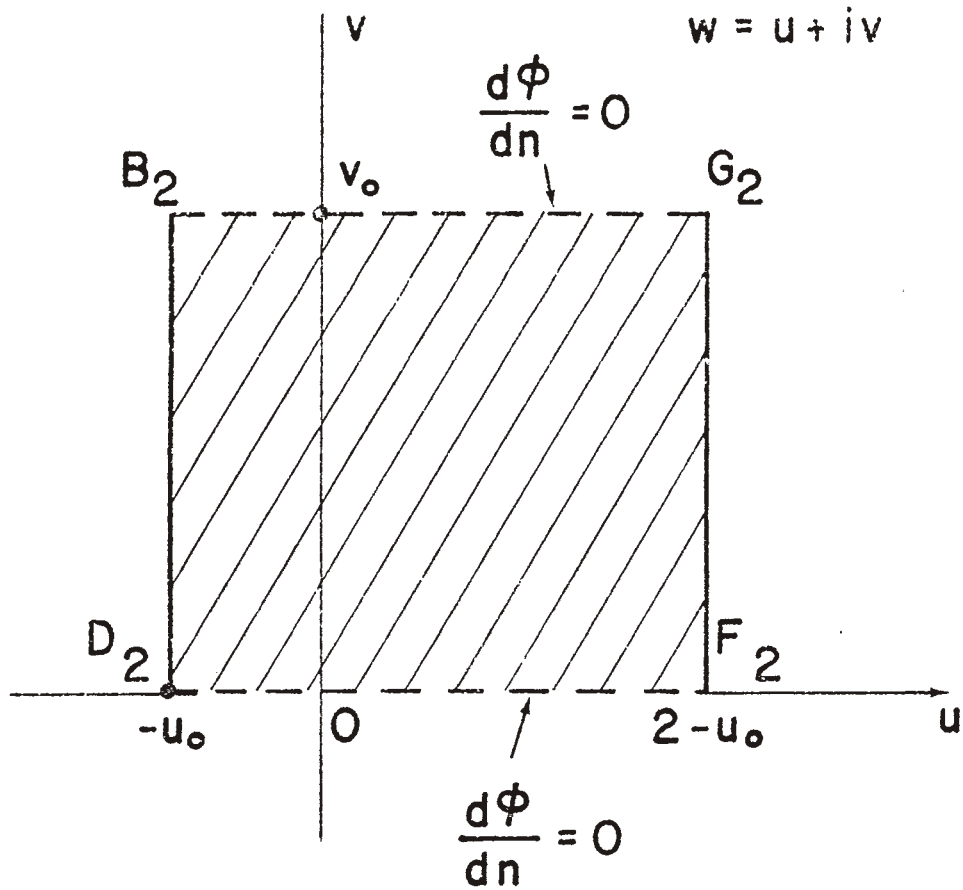
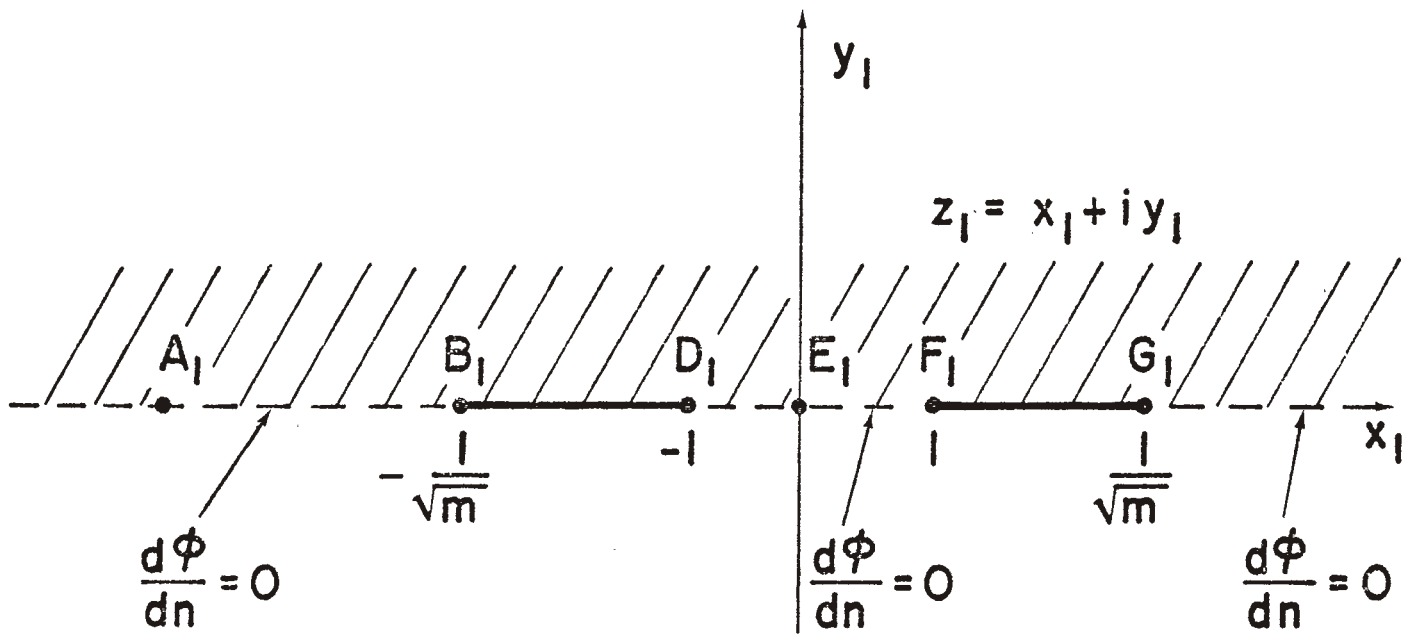


Fig.3. (a) The  $z_1$ -plane containing two strips of equal width and  
 (b) The  $w$ -plane resulting from the Schwarz-Christoffel transformation.

$$m_1 = 1 - m$$

The value  $u_o$  and hence  $Q$  depends on the condition (12d). Equations (6) and (7) show that  $z_1|_{A_1}$  is a real number less than  $-1$ . Hence the value  $\text{sn}^{-1}(z_1|_{A_1}|m)$  in (10) is complex and is given by

$$\text{sn}^{-1}\left(\frac{1}{1+2c_o/d} \middle| m\right) = \text{sn}^{-1}([1 + 2c_o/d]m^{-1/2}|m) + iK(m_1)$$

Thus

$$Q = \text{sn}^{-1}([1 + 2c_o/d]m^{-1/2}|m)/K(m)$$

$$u_o = 1 + \text{sn}^{-1}([1 + 2c_o/d]m^{-1/2}|m)/K(m) \quad (15)$$

and

$$v_1 = v_o$$

The transformation is thus

$$w(z_1) = \left[ \text{sn}^{-1}(z_1|m) - \text{sn}^{-1}([1 + 2c_o/d]m^{-1/2}|m) \right] / K(m) \quad (16)$$

Transformation (16) maps the upper half of the  $z$ -plane into the interior of the rectangle in the  $w$ -plane. The transformation corresponds to the condition of two strips being biased at a potential difference of 2 units: one at potential  $-u_o$  and the other at  $2 - u_o$ , with respect to infinity. The geometrical impedance factor  $f_g$  [2] is defined such that the characteristic impedance  $Z_c$  of the transmission line is given by

$$Z_c = f_g Z \quad (17)$$

where  $Z$  is the intrinsic impedance of the medium. The capacitance  $C$  of the transmission line is related to  $f_g$  by

$$C = \epsilon/f_g \quad (18)$$

where  $\epsilon$  is the dielectric constant of the medium. Thus the geometrical impedance factor can be found by evaluating the capacitance of the configuration; for this problem, it is given, in the  $w$ -plane, by

$$f_g = \frac{1}{2} (\Delta u / \Delta v)$$

where  $\Delta u$  is the potential difference between the two strips and  $\Delta v$  is the change in the field line function on a path encircling one strip. The factor  $1/2$  accounts for the fact that only half of the  $z_1$ -plane maps into the interior of the rectangular region in the  $w$ -plane. Thus

$$f_g = K(m) / K(m_1) \quad (19)$$

For the two strips biased at a potential difference of  $2V$ , the relevant equations are summarized as follows:

$$z_1(z) = \frac{z + c_0}{(1 + 2c_0/d)z - c_0} \quad (20)$$

$$c_0 = \{-a(b + d) + [ab(a + d)(b + d)]^{1/2}\} / (a - b) \quad \text{for } a \neq b \quad (21a)$$

$$= -d/2 \quad \text{for } a = b \quad (21b)$$

$$w(z_1) = V \left[ \text{sn}^{-1}(z_1 | m) - \text{sn}^{-1}([1 + 2c_0/d] m^{-1/2} | m) \right] / K(m) \quad (22)$$

$$f_g = K(m) / K(m_1) \quad (23)$$

where

$$m = [z_1(-a)]^{-2} \quad (24)$$

and

$$m_1 = 1 - m \quad (25)$$

The strip with width  $a$  is at a potential

$$V_a = -V \operatorname{sn}^{-1}([1 + 2c_o/d]m^{-1/2}|m)/K(m) - V \quad (26)$$

and the strip with width  $b$  is at a potential

$$V_b = -V \operatorname{sn}^{-1}([1 + 2c_o/d]m^{-1/2}|m)/K(m) + V \quad (27)$$

In Fig. 4,  $f_g$  is plotted versus  $a/d$  with  $b/d$  as a parameter for two ranges of  $a/d$  ( $0.1 \rightarrow 1$  and  $1 \rightarrow 10$ ). The case  $a = b$  is also presented (the dashed curve). For small values of  $a/d$ ,  $f_g$  values are large, implying small capacitances. For large values of  $a/d$ ,  $f_g$  values quickly approach the limiting values for  $a/d \rightarrow \infty$ . Because of the symmetry in  $a$  and  $b$ , the curve  $b/d \rightarrow \infty$  can be used to specify these limiting values of  $f_g$ : e.g., the  $f_g$  value at  $a/d = 5$  and  $b/d \rightarrow \infty$  indicates that the limiting value of  $f_g$  for  $b/d = 5$  is 0.351.

The  $f_g$  values are also tabulated in Table I to Table IV for four ranges of  $a/d$  ( $0.01 \rightarrow 0.1$ ,  $0.1 \rightarrow 1$ ,  $1 \rightarrow 10$ , and  $10 \rightarrow 100$ ). As expected, when both strips are infinitely wide,  $f_g \rightarrow 0$ , i.e., there is an infinite capacitance between the two strips.

The field and potential distributions of the two coplanar strips can be obtained by evaluating (20) - (27). As mentioned earlier, the two strips have equal but opposite charges. However, the potentials of the two strips are given by (26) and (27), and they are not equal in magnitude with respect to infinity except in the equal width case. The potential difference is given by

$$V_b - V_a = 2V.$$

In Fig. 5 to Fig. 14, we present the plots of the field and potential distributions for ten different geometries. In these plots, the solid curves (————) represent equi-potential lines and these curves are plotted in potential increments of  $0.1V$ . The dashed curves (-----) represent the field lines, and the dash-dotted curves (-.-.-) represent the zero potential lines. These ten plots cover a wide range of strip widths and strip separation and provide an understanding of the field distributions in this kind of structure.

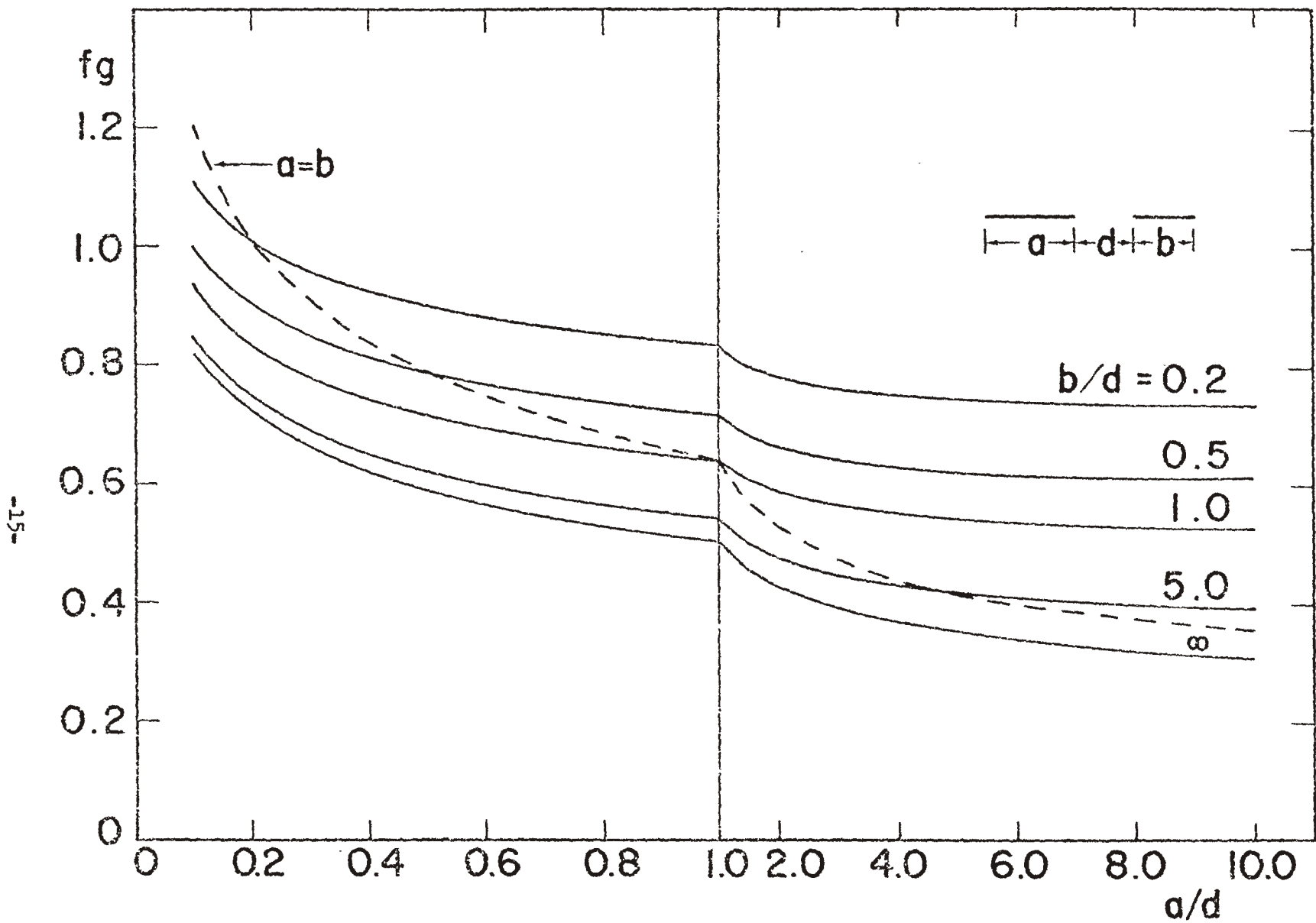


Fig.4. The geometrical impedance factor versus  $a/d$  with  $b/d$  as a parameter. The case  $a = b$  is also plotted. Note the change in abscissa scale.

Table I. The geometrical impedance factor for  $a/d \leq 0.1$

$a/d \backslash b/d$	0.00001	0.2	0.5	1	2	5	10	$\infty$
0.00001	4.10595	2.55876	2.44844	2.38390	2.33812	2.30260	2.28875	2.27358
0.010	3.00812	1.46082	1.35037	1.28571	1.23979	1.20414	1.19023	1.17499
0.015	2.94438	1.39701	1.28649	1.22177	1.17578	1.14007	1.12613	1.11086
0.020	2.89937	1.35194	1.24136	1.17657	1.13052	1.09474	1.08078	1.06546
0.025	2.86463	1.31714	1.20650	1.14164	1.09553	1.05969	1.04569	1.03034
0.030	2.83639	1.28884	1.17813	1.11321	1.06703	1.03113	1.01710	1.00172
0.035	2.81263	1.26501	1.15424	1.08926	1.04302	1.00705	0.99299	0.97757
0.040	2.79214	1.24446	1.13363	1.06859	1.02228	0.98625	0.97216	0.95671
0.045	2.77416	1.22642	1.11553	1.05042	1.00405	0.96795	0.95384	0.93835
0.050	2.75815	1.21035	1.09940	1.03422	0.98779	0.95163	0.93749	0.92196
0.055	2.74374	1.19588	1.08486	1.01963	0.97314	0.93691	0.92274	0.90717
0.060	2.73064	1.18272	1.07165	1.00635	0.95980	0.92351	0.90930	0.89371
0.065	2.71865	1.17067	1.05954	0.99418	0.94756	0.91121	0.89698	0.88135
0.070	2.70760	1.15956	1.04837	0.98295	0.93627	0.89986	0.88560	0.86993
0.075	2.69736	1.14927	1.03801	0.97254	0.92580	0.88932	0.87503	0.85932
0.080	2.68783	1.13968	1.02837	0.96283	0.91603	0.87948	0.86516	0.84943
0.085	2.67891	1.13071	1.01934	0.95374	0.90688	0.87027	0.85592	0.84015
0.090	2.67055	1.12228	1.01086	0.94520	0.89828	0.86161	0.84723	0.83143
0.095	2.66267	1.11435	1.00287	0.93715	0.89017	0.85344	0.83903	0.82319
0.100	2.65523	1.10686	0.99532	0.92954	0.88250	0.84571	0.83127	0.81540



Table II. The geometrical impedance factor for  $0.1 \leq a/d \leq 1$

$a/d \backslash b/d$	0.00001	0.2	0.5	1	2	5	10	$\infty$
0.10	2.65523	1.10686	0.99532	0.92954	0.88250	0.84571	0.83127	0.81540
0.15	2.59777	1.04887	0.93678	0.87044	0.82281	0.78541	0.77070	0.75448
0.20	2.55876	1.00937	0.89677	0.82989	0.78171	0.74373	0.72874	0.71218
0.25	2.52974	0.97990	0.86682	0.79944	0.75072	0.71218	0.69693	0.68004
0.30	2.50697	0.95671	0.84318	0.77532	0.72610	0.68701	0.67150	0.65429
0.35	2.48844	0.93779	0.82384	0.75554	0.70582	0.66621	0.65044	0.63291
0.40	2.47297	0.92196	0.80762	0.73889	0.68871	0.64859	0.63257	0.61473
0.45	2.45981	0.90846	0.79375	0.72461	0.67398	0.63337	0.61711	0.59896
0.50	2.44844	0.89677	0.78171	0.71218	0.66113	0.62004	0.60354	0.58509
0.55	2.43849	0.88652	0.77112	0.70123	0.64977	0.60821	0.59148	0.57273
0.60	2.42969	0.87744	0.76174	0.69149	0.63964	0.59763	0.58067	0.56163
0.65	2.42185	0.86934	0.75333	0.68276	0.63052	0.58807	0.57089	0.55156
0.70	2.41481	0.86204	0.74576	0.67486	0.62226	0.57938	0.56199	0.54237
0.75	2.40844	0.85544	0.73889	0.66769	0.61473	0.57144	0.55383	0.53393
0.80	2.40265	0.84943	0.73262	0.66113	0.60783	0.56414	0.54632	0.52614
0.85	2.39736	0.84393	0.72688	0.65511	0.60148	0.55739	0.53937	0.51891
0.90	2.39251	0.83887	0.72159	0.64955	0.59561	0.55114	0.53291	0.51219
0.95	2.38804	0.83421	0.71671	0.64441	0.59016	0.54532	0.52689	0.50590
1.00	2.38390	0.82989	0.71218	0.63964	0.58509	0.53988	0.52126	0.50001

Table III. The geometrical impedance factor for  $1 \leq a/d \leq 10$

a/d \ b/d	0.00001	0.2	0.5	1	2	5	10	$\infty$
1.0	2.38390	0.82989	0.71218	0.63964	0.58509	0.53988	0.52126	0.50001
1.5	2.35489	0.79944	0.68004	0.60546	0.54840	0.50001	0.47962	0.45588
2.0	2.33812	0.78171	0.66113	0.58509	0.52614	0.47517	0.45327	0.42730
2.5	2.32714	0.77003	0.64859	0.57144	0.51101	0.45793	0.43472	0.40669
3.0	2.31937	0.76174	0.63964	0.56163	0.50001	0.44515	0.42078	0.39085
3.5	2.31358	0.75554	0.63291	0.55421	0.49161	0.43524	0.40984	0.37815
4.0	2.30910	0.75072	0.62768	0.54840	0.48499	0.42730	0.40098	0.36763
4.5	2.30552	0.74687	0.62348	0.54373	0.47962	0.42078	0.39364	0.35872
5.0	2.30260	0.74373	0.62004	0.53988	0.47517	0.41533	0.38743	0.35104
5.5	2.30017	0.74111	0.61716	0.53666	0.47143	0.41069	0.38210	0.34431
6.0	2.29812	0.73889	0.61473	0.53393	0.46824	0.40669	0.37747	0.33835
6.5	2.29636	0.73698	0.61264	0.53157	0.46548	0.40321	0.37341	0.33302
7.0	2.29484	0.73534	0.61082	0.52953	0.46308	0.40015	0.36981	0.32820
7.5	2.29350	0.73389	0.60923	0.52773	0.46096	0.39743	0.36660	0.32382
8.0	2.29233	0.73262	0.60783	0.52614	0.45907	0.39500	0.36371	0.31982
8.5	2.29129	0.73149	0.60658	0.52472	0.45739	0.39282	0.36110	0.31613
9.0	2.29035	0.73048	0.60546	0.52345	0.45588	0.39085	0.35872	0.31272
9.5	2.28951	0.72956	0.60445	0.52230	0.45452	0.38906	0.35655	0.30955
10.0	2.28875	0.72874	0.60354	0.52126	0.45327	0.38743	0.35456	0.30660

Table IV. The geometrical impedance for  $a/d \geq 10$

$a/d \backslash b/d$	0.00001	0.2	0.5	1	2	5	10	$\infty$
10	2.28875	0.72874	0.60354	0.52126	0.45327	0.38743	0.35456	0.30660
15	2.28386	0.72341	0.59763	0.51451	0.44515	0.37653	0.34102	0.28492
20	2.28135	0.72068	0.59459	0.51101	0.44090	0.37067	0.33351	0.27116
25	2.27983	0.71901	0.59273	0.50888	0.43828	0.36701	0.32871	0.26131
30	2.27880	0.71789	0.59148	0.50743	0.43651	0.36450	0.32538	0.25375
35	2.27807	0.71709	0.59059	0.50640	0.43524	0.36268	0.32292	0.24768
40	2.27751	0.71649	0.58991	0.50561	0.43427	0.36129	0.32104	0.24264
45	2.27708	0.71601	0.58938	0.50500	0.43351	0.36020	0.31954	0.23835
50	2.27674	0.71563	0.58896	0.50451	0.43290	0.35931	0.31833	0.23464
55	2.27645	0.71532	0.58861	0.50410	0.43240	0.35859	0.31733	0.23138
60	2.27621	0.71506	0.58832	0.50377	0.43198	0.35798	0.31648	0.22847
65	2.27601	0.71484	0.58807	0.50348	0.43163	0.35746	0.31576	0.22586
70	2.27584	0.71466	0.58786	0.50324	0.43132	0.35701	0.31513	0.22350
75	2.27569	0.71449	0.58768	0.50302	0.43106	0.35662	0.31459	0.22134
80	2.27556	0.71435	0.58752	0.50284	0.43083	0.35628	0.31411	0.21936
85	2.27545	0.71422	0.58737	0.50267	0.43062	0.35598	0.31369	0.21753
90	2.27534	0.71411	0.58725	0.50252	0.43044	0.35571	0.31331	0.21583
95	2.27525	0.71401	0.58713	0.50239	0.43028	0.35547	0.31297	0.21425
100	2.27517	0.71392	0.58703	0.50227	0.43013	0.35525	0.31266	0.21277
$\infty$	2.27358	0.71218	0.58509	0.50001	0.42730	0.35104	0.30660	0

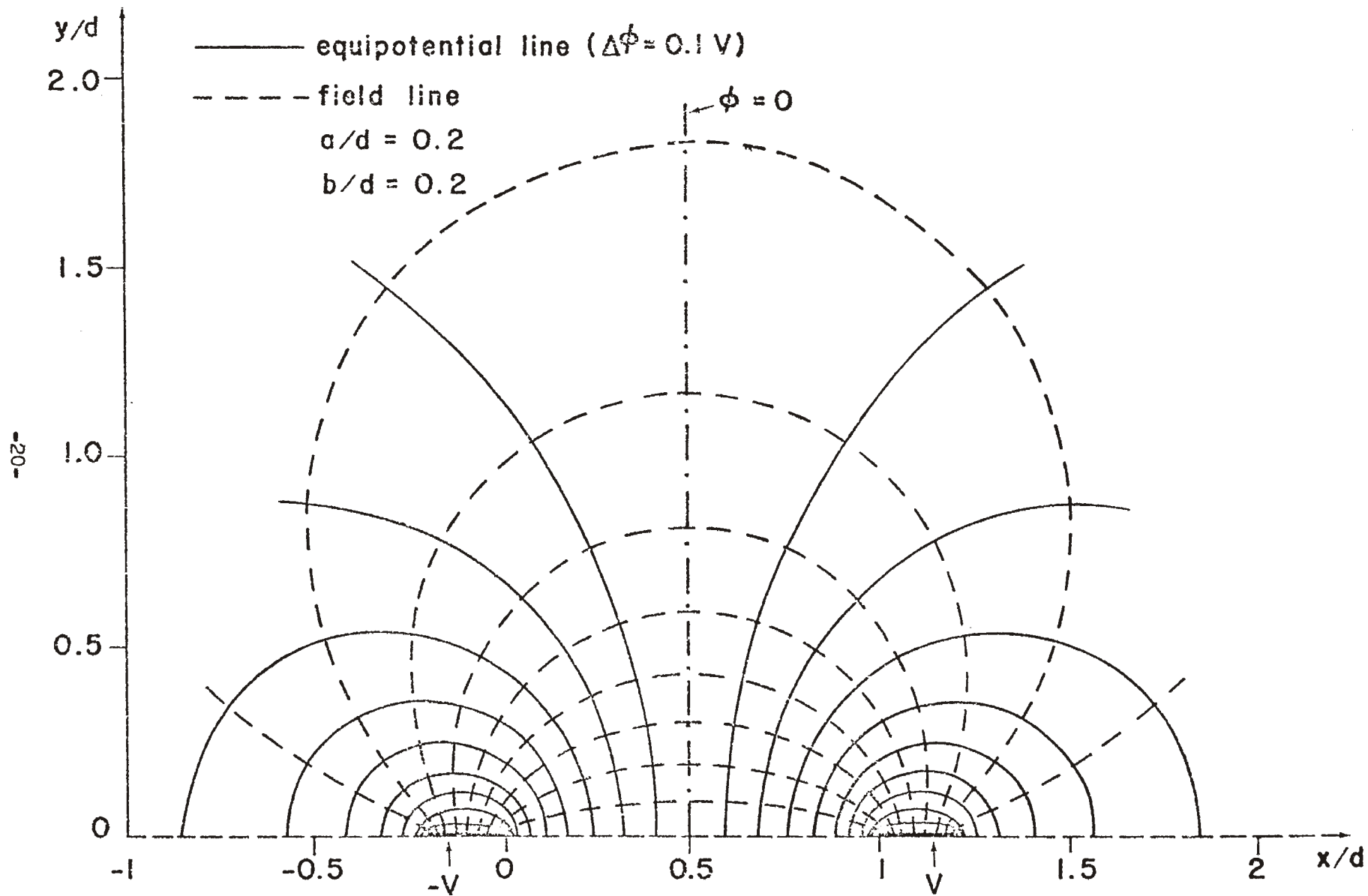


Fig.5. Field distribution of the two coplanar strips.  $a/d = 0.2$ ,  $b/d = 0.2$ .

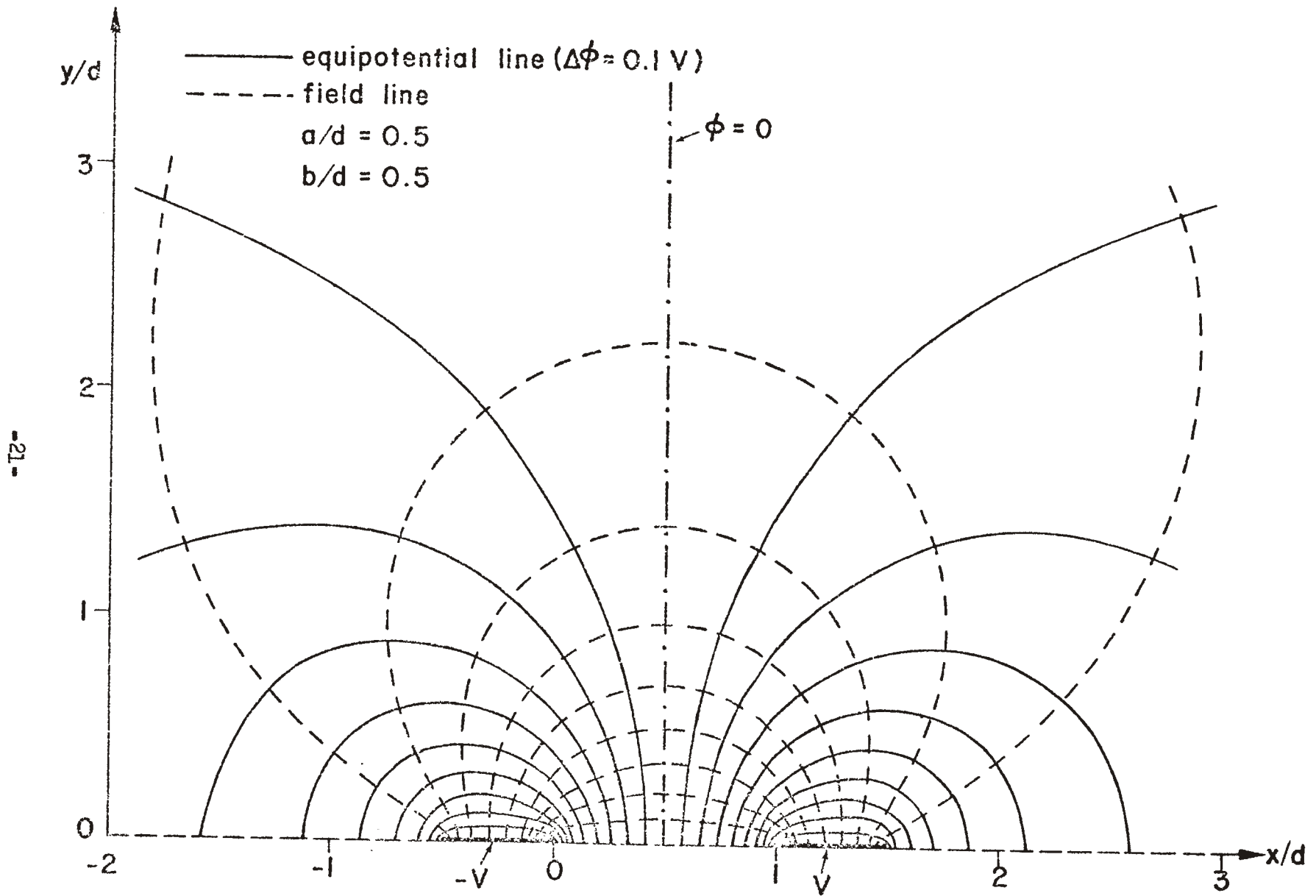


Fig.6. Field distribution of the two coplanar strips.  $a/d = 0.5$ ,  $b/d = 0.5$ .

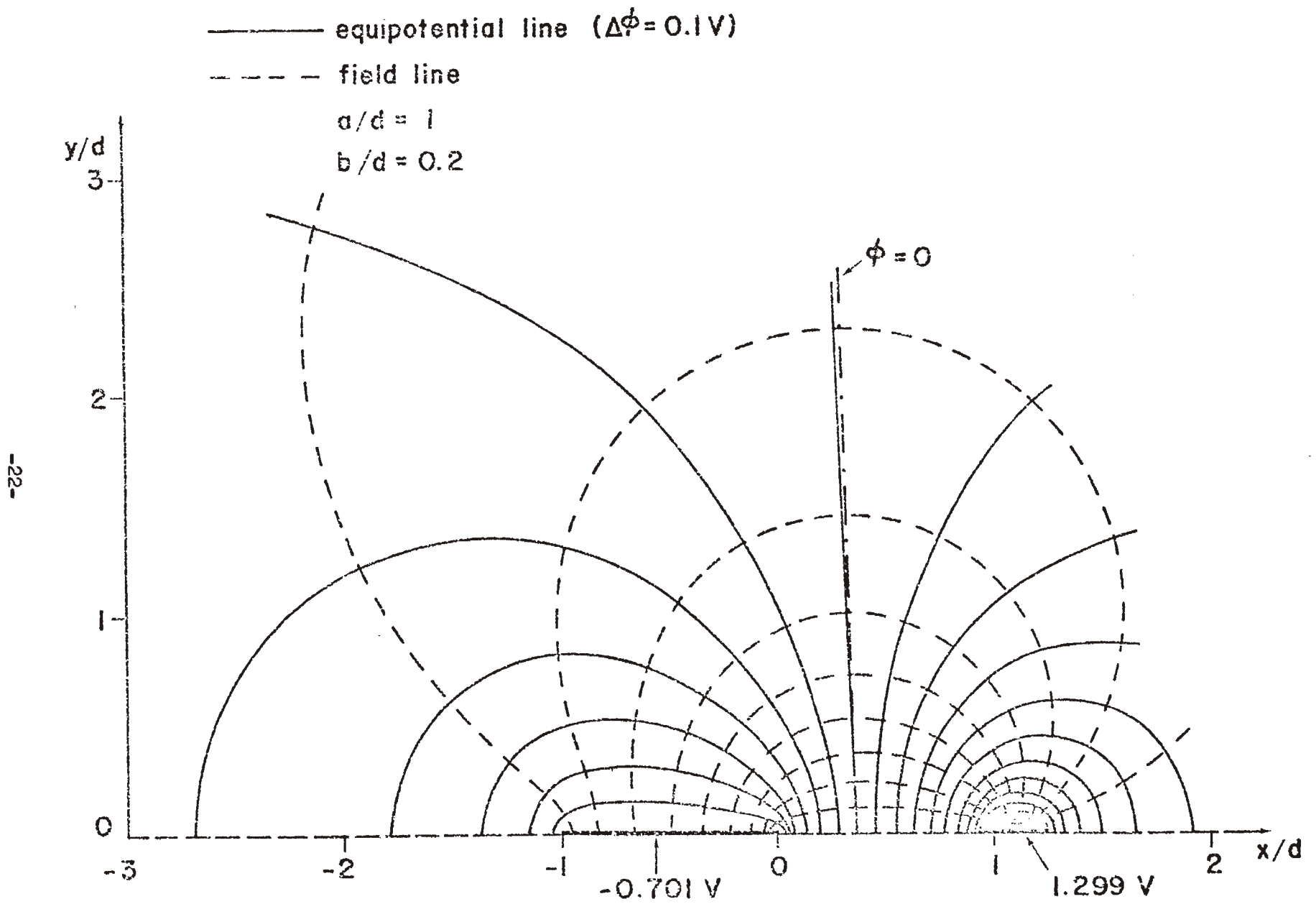


Fig.7. Field distribution of the two coplanar strips.  $a/d = 1$ ,  $b/d = 0.2$ .

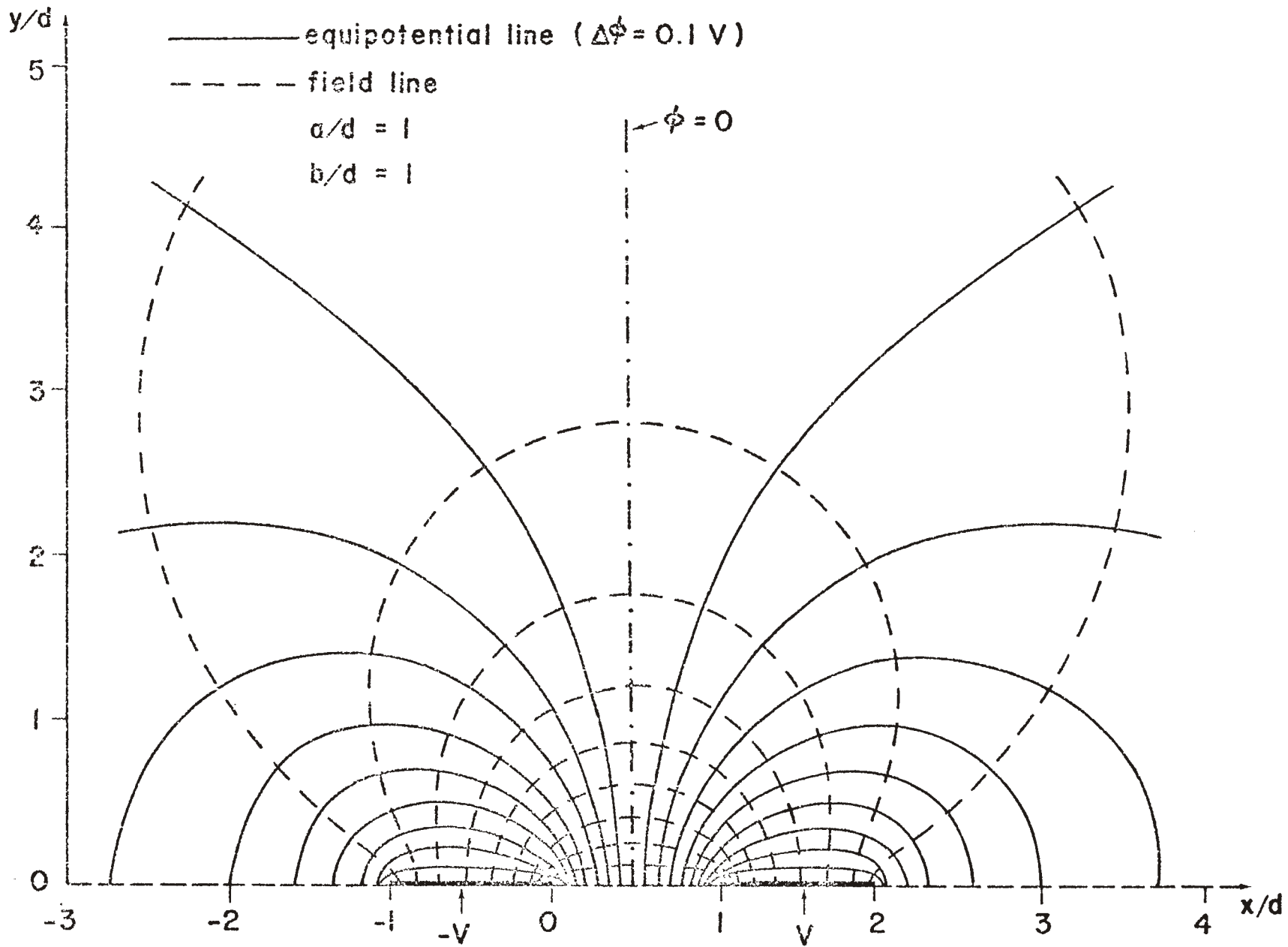


Fig.8. Field distribution of the two coplanar strips.  $a/d = 1$ ,  $b/d = 1$ .

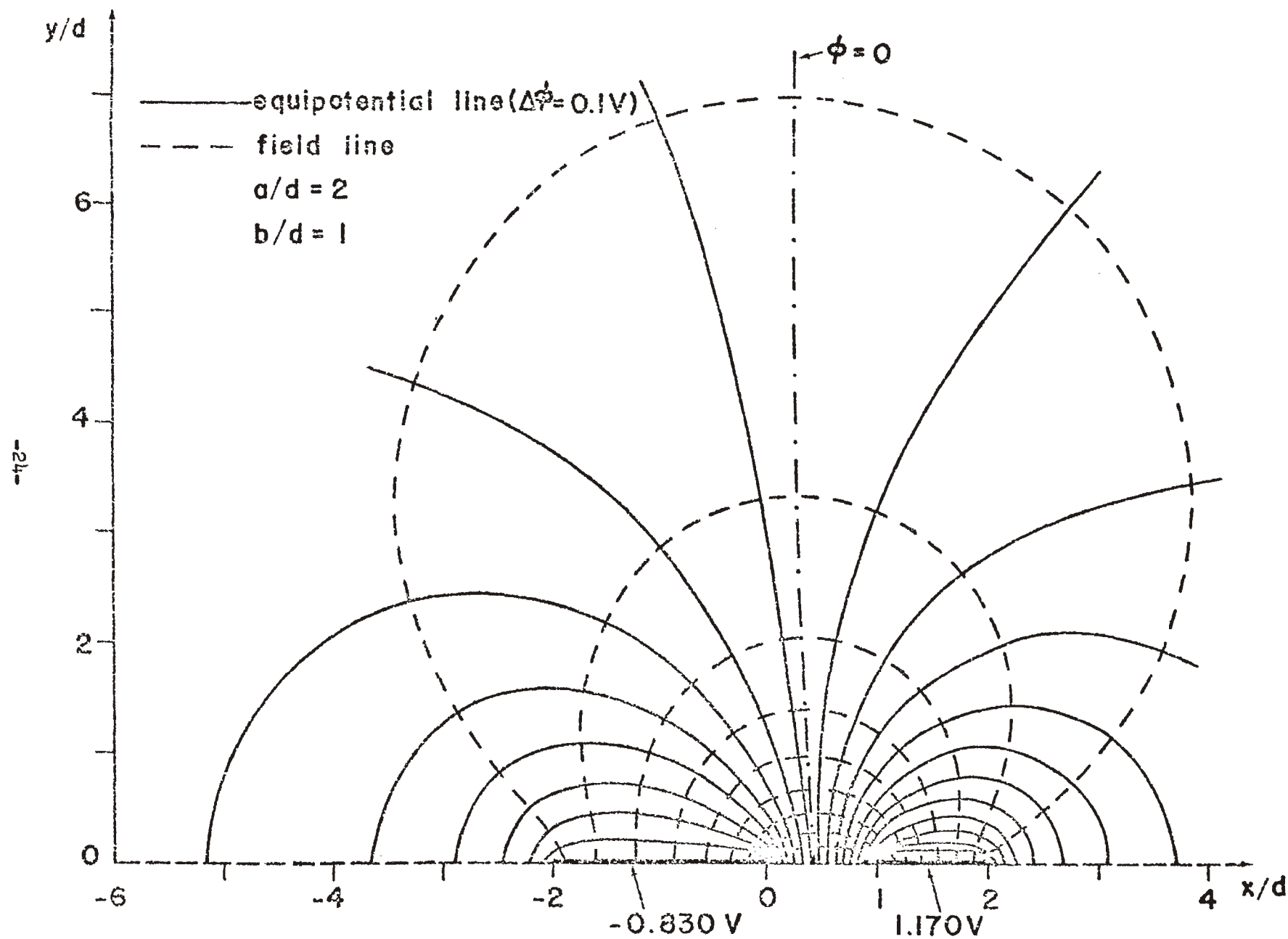


Fig.9. Field distribution of the two coplanar strips.  $a/d = 2$ ,  $b/d = 1$ .



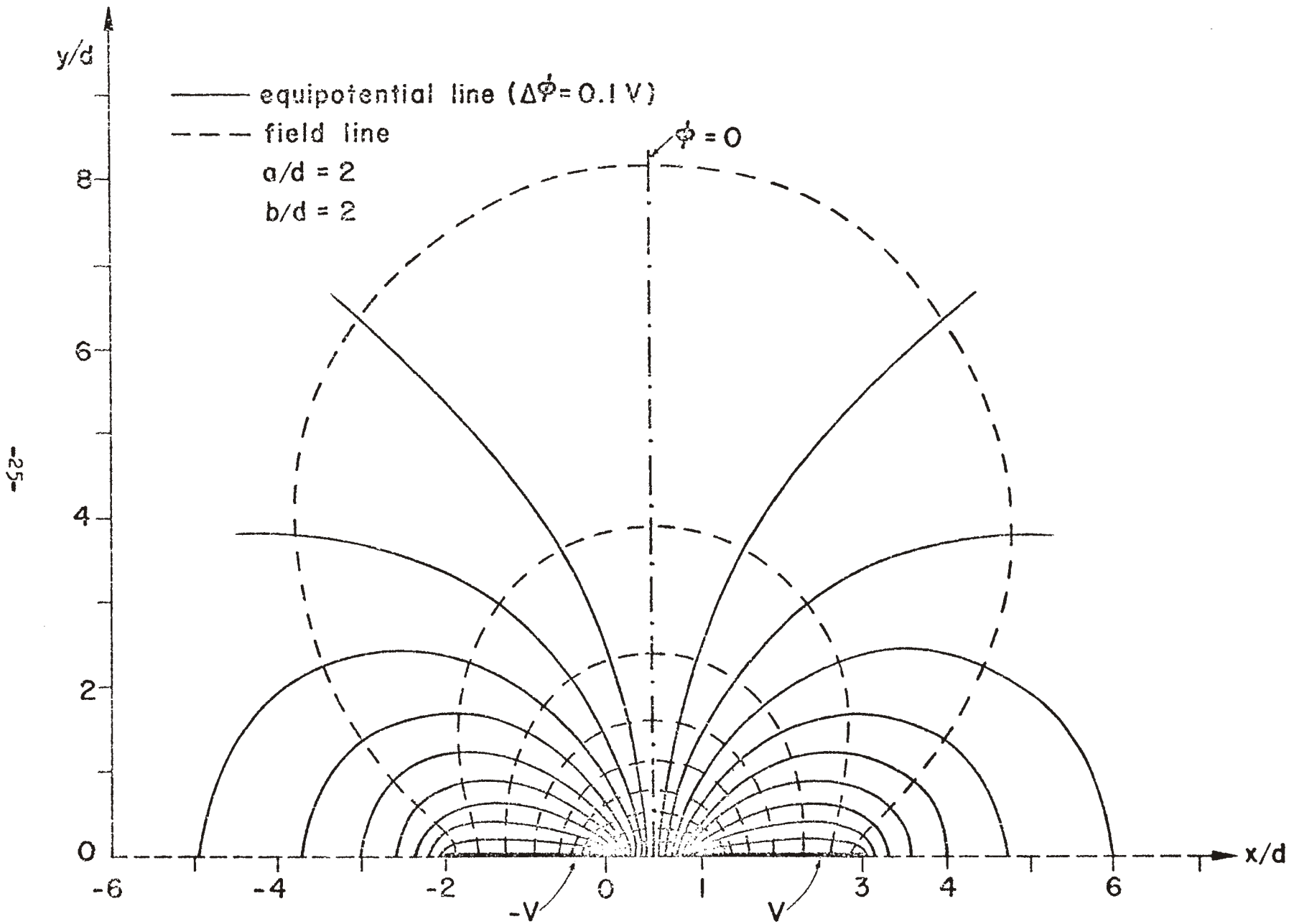


Fig.10. Field distribution of the two coplanar strips.  $a/d = 2$ ,  $b/d = 2$ .

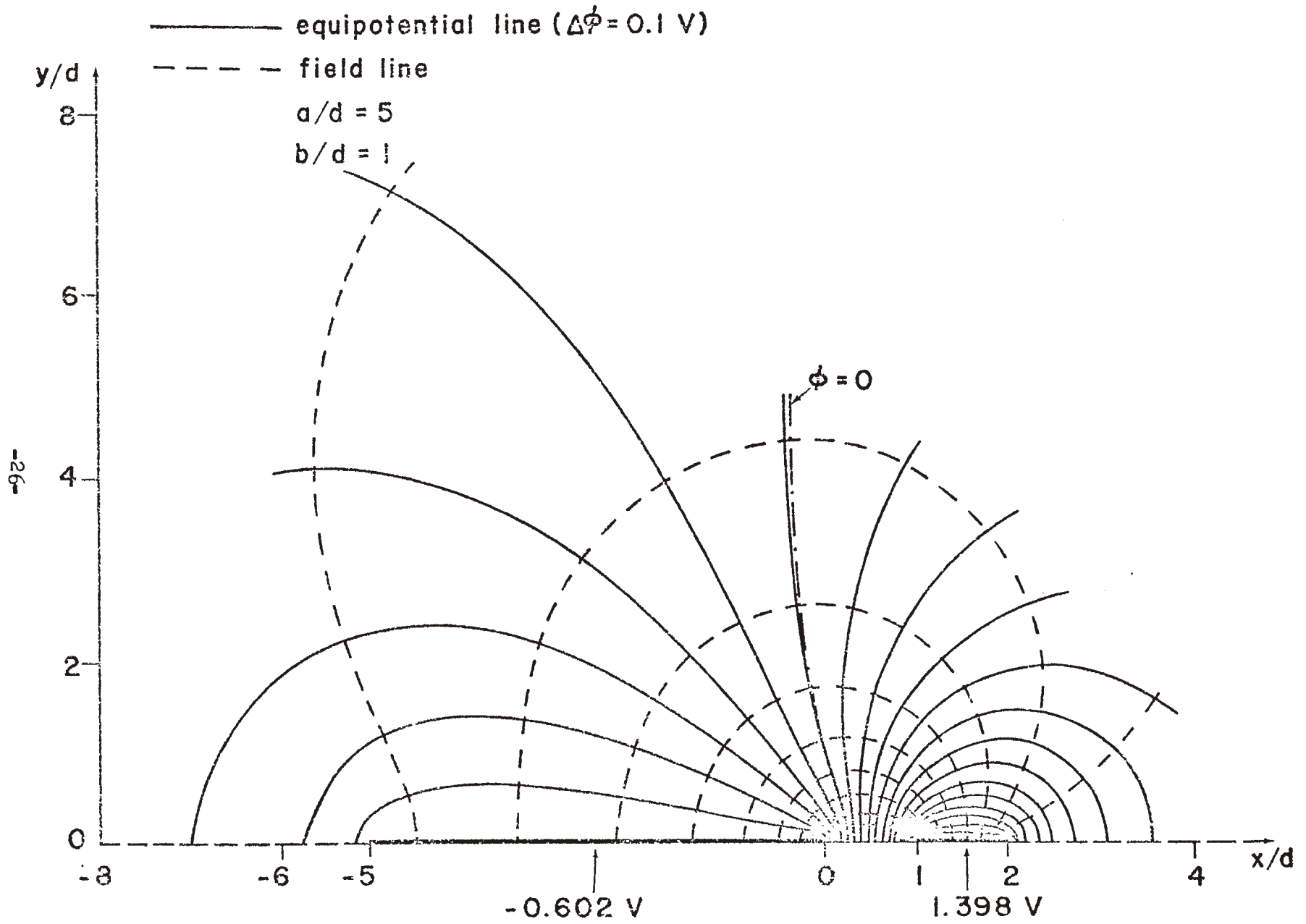


Fig.11. Field distribution of the two coplanar strips.  $a/d = 5$ ,  $b/d = 1$ .

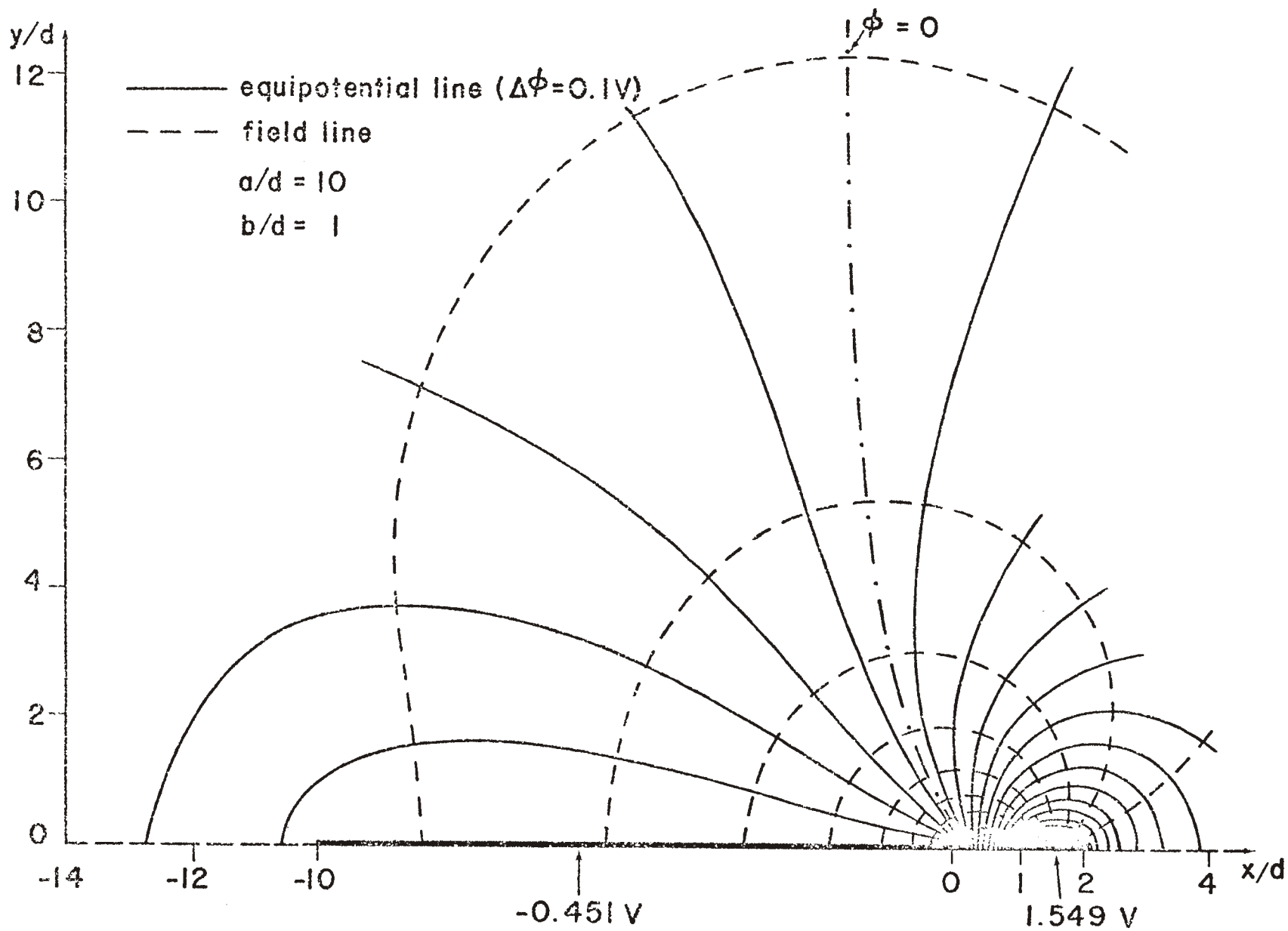


Fig.12. Field distribution of the two coplanar strips.  $a/d = 10$ ,  $b/d = 1$ .

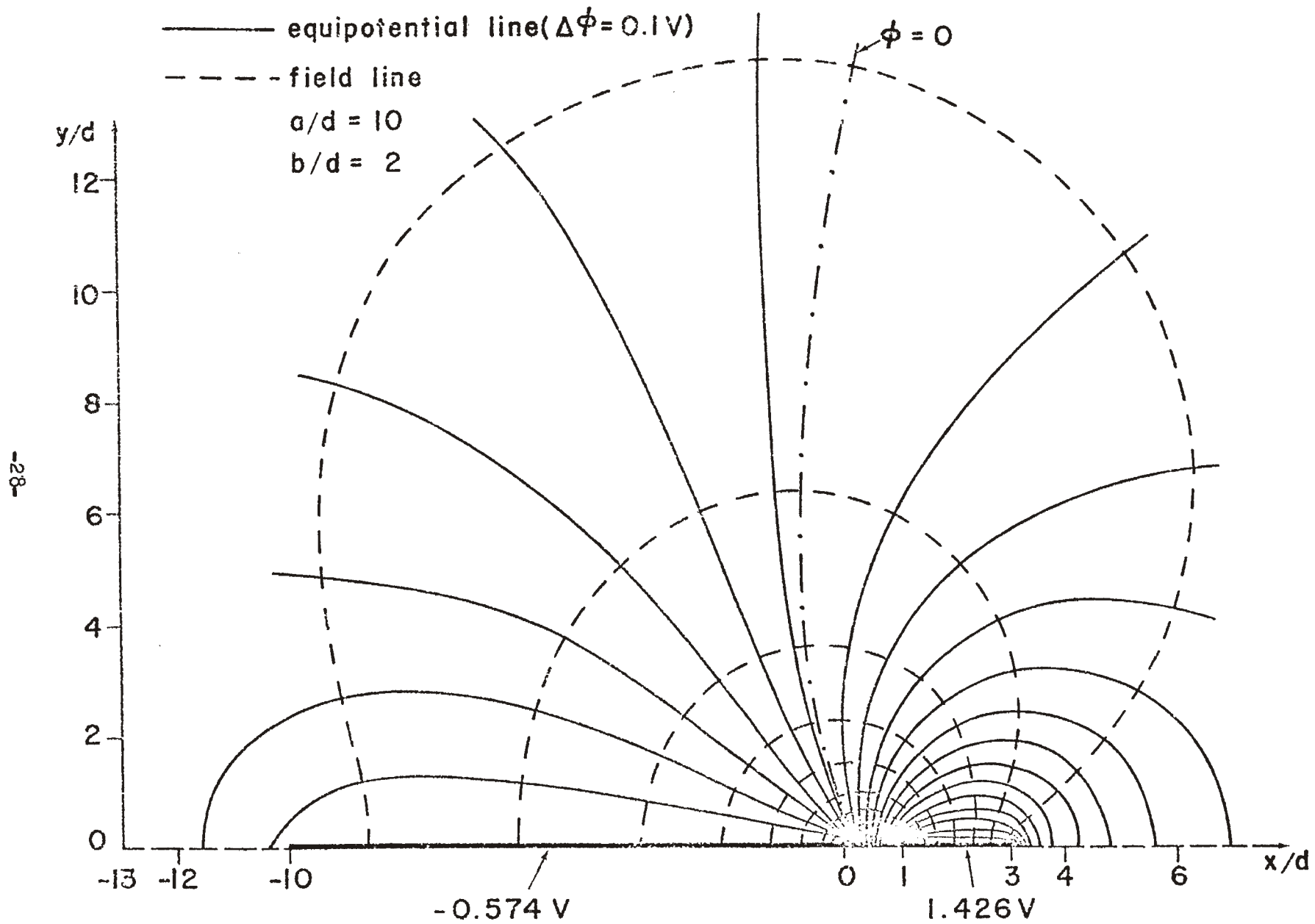


Fig.13. Field distribution of the two coplanar strips.  $a/d = 10$ ,  $b/d = 2$ .

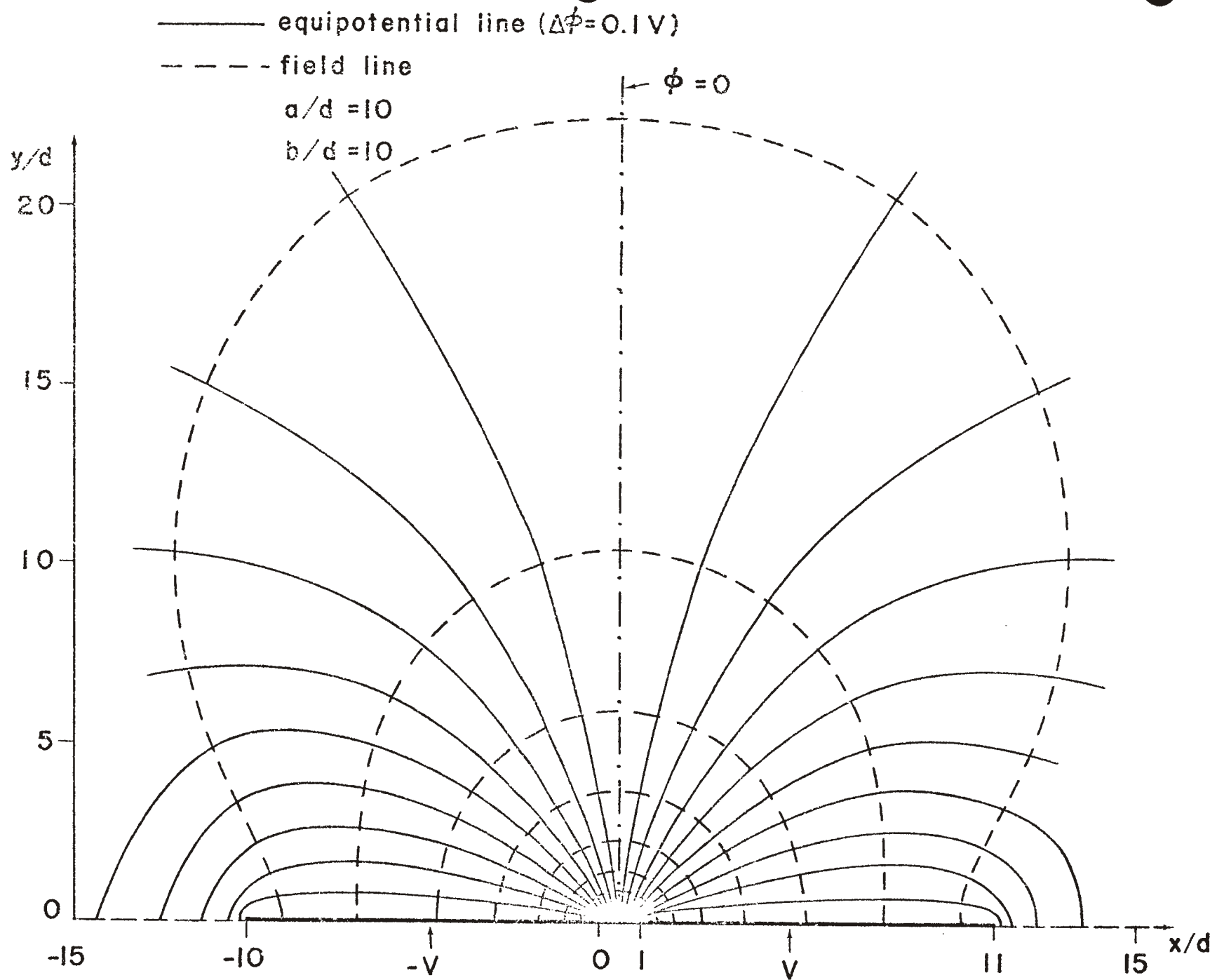


Fig.14. Field distribution of the two coplanar strips.  $a/d = 10$ ,  $b/d = 10$ .

### III. Coplanar Strip Lines and Two-Cylinder Transmission Lines

The geometrical impedance factor of the coplanar strip transmission line is compared in this section with that of the transmission line of two parallel circular cylinders.

The configuration of the two-cylinder line is shown in Fig. 15. The cylinders, having radii  $r_1$  and  $r_2$ , have their centers separated by a distance  $s$ . The geometrical impedance factor  $f'_g$  is given by

$$f'_g = (1/2\pi) \cosh^{-1} [(s^2 - r_1^2 - r_2^2)/2r_1r_2] \quad (28)$$

The first case to investigate is that the two cylinder radii are one quarter of the strip widths, and that both transmission lines have their centers equally separated, i.e.,

$$r_1 = (1/4)a \quad (29a)$$

$$r_2 = (1/4)b \quad (29b)$$

and

$$s = d + \frac{1}{2}(a + b) \quad (29c)$$

This configuration is shown in Fig. 16. The reason that conditions (29) are imposed is prompted by previous knowledge that a strip antenna can be represented by a circular cylindrical antenna with an equivalent radius being equal to one quarter of the strip width. However, computed results show that the agreement between (23) and (28) is good only if the strip widths are small compared to the separation. In fact, in the limit of vanishingly small strip widths, the two geometrical impedance factors are exactly equal. This can be shown analytically by taking the asymptotic expressions of (23) and (28). For the strip case, we first find the values of  $m$  and  $m_1$  for  $a/d \rightarrow 0$  and  $b/d \rightarrow 0$ . From (24) and (28), we have

$$\lim_{\substack{a/d \rightarrow 0 \\ b/d \rightarrow 0}} m = [1 - 2\sqrt{ab}/d]^2 \approx 1 \quad (30)$$

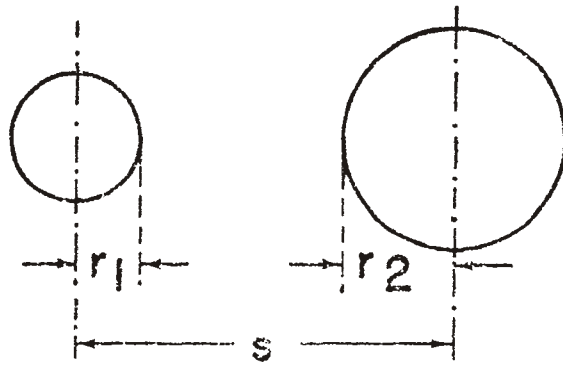


Fig.15. The cross-sectional view of a two-cylinder transmission line.

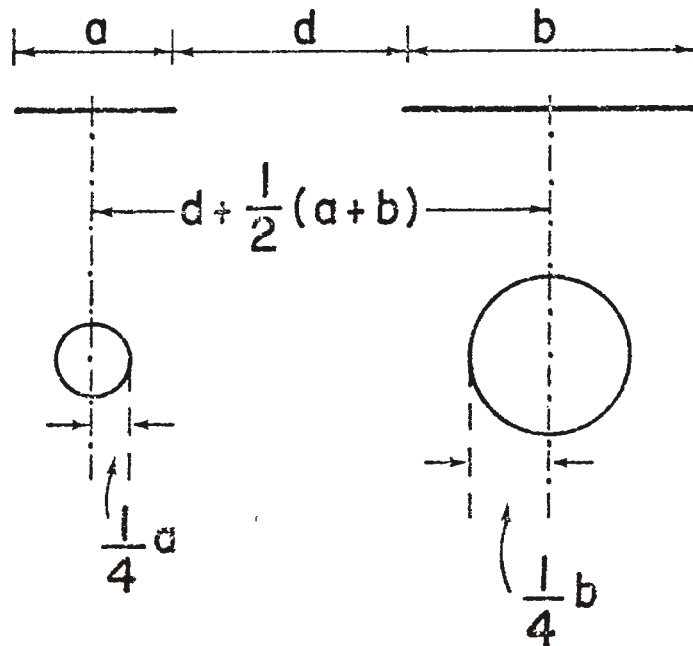


Fig.16. A comparison of the strip transmission line with a two-cylinder transmission line.



and

$$\lim_{\substack{a/d \rightarrow 0 \\ b/d \rightarrow 0}} m_1 = 4\sqrt{ab}/d \approx 0 \quad (31)$$

The asymptotic values [7] of the two complete elliptic integrals are

$$\lim_{m \rightarrow 0} K(m) = \ln(4/m_1)$$

and

$$\lim_{m \rightarrow 0} K(m_1) = \pi/2$$

Thus, the geometrical impedance factor for the vanishingly small strips is

$$\lim_{\substack{a/d \rightarrow 0 \\ b/d \rightarrow 0}} f_g = (1/\pi)[2 \ln 2 - \frac{1}{2} \ln(ab/d^2)] \quad (32)$$

For the cylinder case, using the identity

$$\cosh^{-1} x = \ln(x + \sqrt{x^2 - 1})$$

and

$$\lim_{\substack{a/d \rightarrow 0 \\ b/d \rightarrow 0}} \frac{s^2 - r_1^2 - r_2^2}{2r_1 r_2} = 8d^2/ab$$

we obtain

$$\lim_{\substack{a/d \rightarrow 0 \\ b/d \rightarrow 0}} f'_g = 1/\pi[2 \ln 2 - \frac{1}{2} \ln(ab/d^2)] \quad (33)$$

Equations (32) and (33) show that when the strip widths are vanishingly small compared to the separation, then for equal characteristic impedances, the equivalent radii of the two-cylinder transmission line are equal to one quarter of the strip widths.

In Fig. 17, we present a plot of the two geometrical impedance factors versus  $a/d$  for the condition  $a = b$ . In the same diagram, we also present the percentage difference  $\Delta f_g / f_g$  of the two factors, where

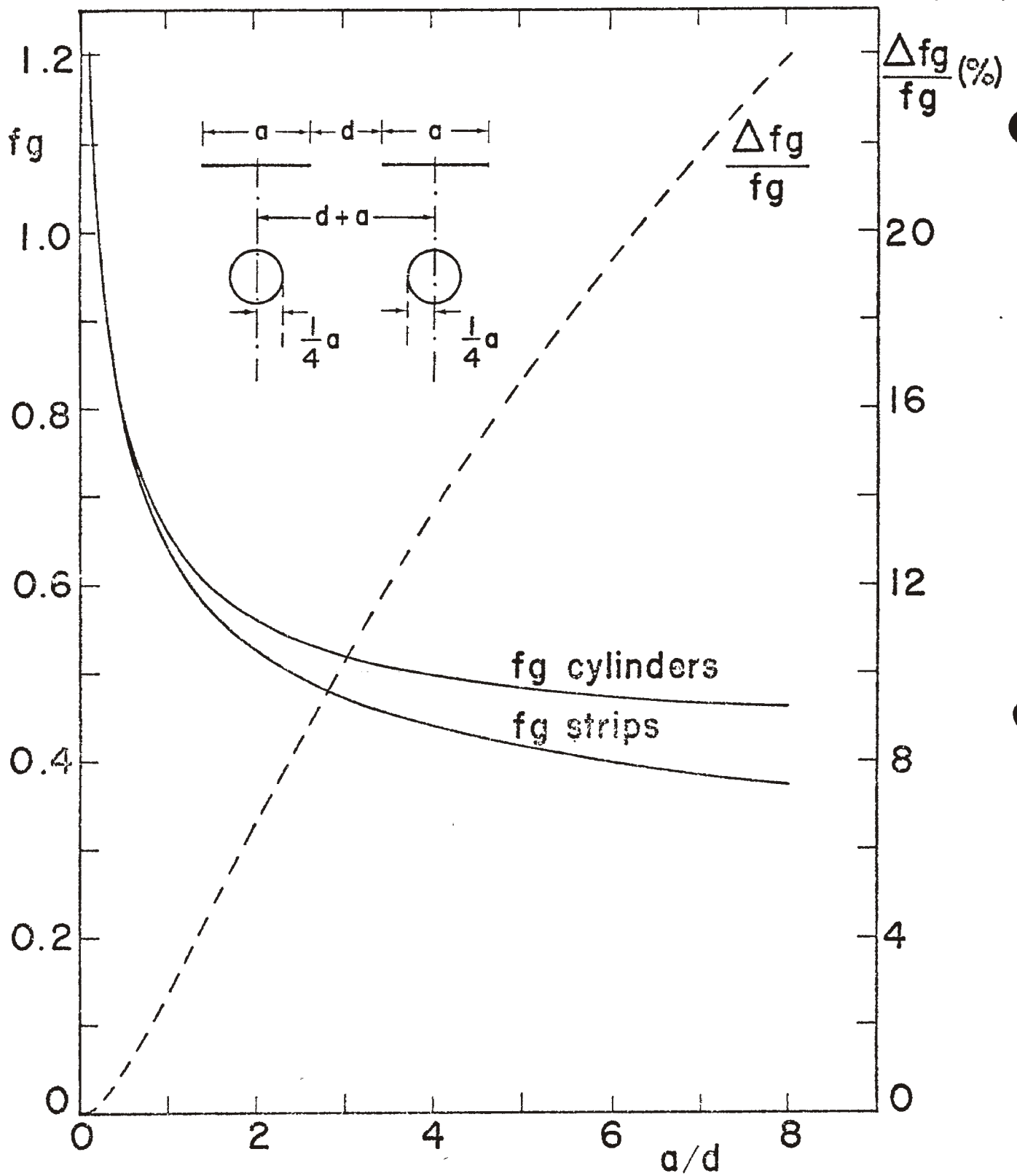


Fig.17. The geometrical impedance factor of a strip transmission line of equal strip width and of a two-cylinder line with the cylinder radii equal to one quarter of the strip width. The percentage difference of the two factors is shown as the dashed line.

$$\Delta f_g / f_g = (f'_g - f_g) / f_g \times 100\%$$

We observe that for a 5% difference in the two factors,  $a/d$  is about 1.6. For large values of  $a/d$ , the two-cylinder configuration with conditions (29) is not a good representation of the strips.

- - - - -

The second case we investigate is that the cylinders have diameters equal to the strip widths and are separated by the same distance, i.e.,

$$r_1 = (1/2)a \tag{34a}$$

$$r_2 = (1/2)b \tag{34b}$$

and

$$s = d + \frac{1}{2}(a + b) \tag{34c}$$

This configuration is shown in Fig. 18. Computed results show that the two geometrical factors differ approximately by a constant value over a wide range of  $a/d$  and  $b/d$  values. We can calculate this constant value by finding the difference of the two factors at small values of  $a/d$  and  $b/d$ . With conditions (34), we have

$$\lim_{\substack{a/d \rightarrow 0 \\ b/d \rightarrow 0}} \frac{s^2 - r_1^2 - r_2^2}{2r_1 r_2} = 2d^2/ab$$

The geometrical impedance factor is thus given by

$$\lim_{\substack{a/d \rightarrow 0 \\ b/d \rightarrow 0}} f'_g = (1/\pi) [\ln 2 - \frac{1}{2} \ln(ab/d^2)] \tag{35}$$

The difference  $D_o$  of the two geometrical impedance factors is

$$D_o = \lim_{\substack{a/d \rightarrow 0 \\ b/d \rightarrow 0}} (f_g - f'_g) = (1/\pi) \ln 2 = 0.220636 \tag{36}$$

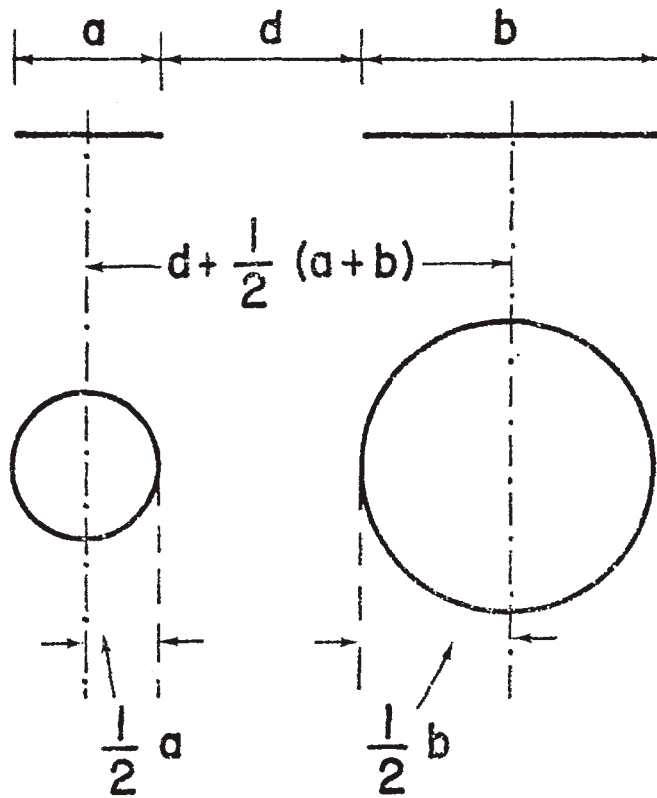


Fig.18. A comparison of the strip transmission line with a two-cylinder transmission line.

In Fig. 19, we present a plot of  $f_g$  and  $f'_g$  versus  $a/d$  for the case  $a = b$ . We also present a plot of the percentage difference of  $D_o$  and  $f_g - f'_g$ , as defined by

$$\delta_f = [D_o - (f_g - f'_g)]/D_o \times 100\% \quad (37)$$

We observe that  $\delta_f$  is small, i.e., the two factors,  $f_g$  and  $f'_g$  differ approximately by the value  $D_o$  given by (36). In Fig. 20, we present a graph of  $\delta_f$  versus  $a/d$  with  $b/d$  as a parameter. For  $a/d < 8$ ,  $\delta_f$  is within about 5% even when  $b/d \rightarrow \infty$ . We thus conclude that for one strip being less than eight times the separation between the inner edges of the strips, the geometrical impedance factor of the two coplanar strip line is approximately equal to that of a two-cylinder line plus a constant value of 0.22064. The two-cylinder line satisfies conditions (34), i.e. the cylinder diameters equal to the strip widths, and the cylinders have the same separation as the strips. We summarize this in the following expression

$$f_g|_{\text{strips}} = f_g|_{\text{2-cylinder}} + 0.22064 \quad (38)$$

This above formula is useful because the geometrical impedance factor of the two-cylinder transmission line can be easily calculated or found in references.

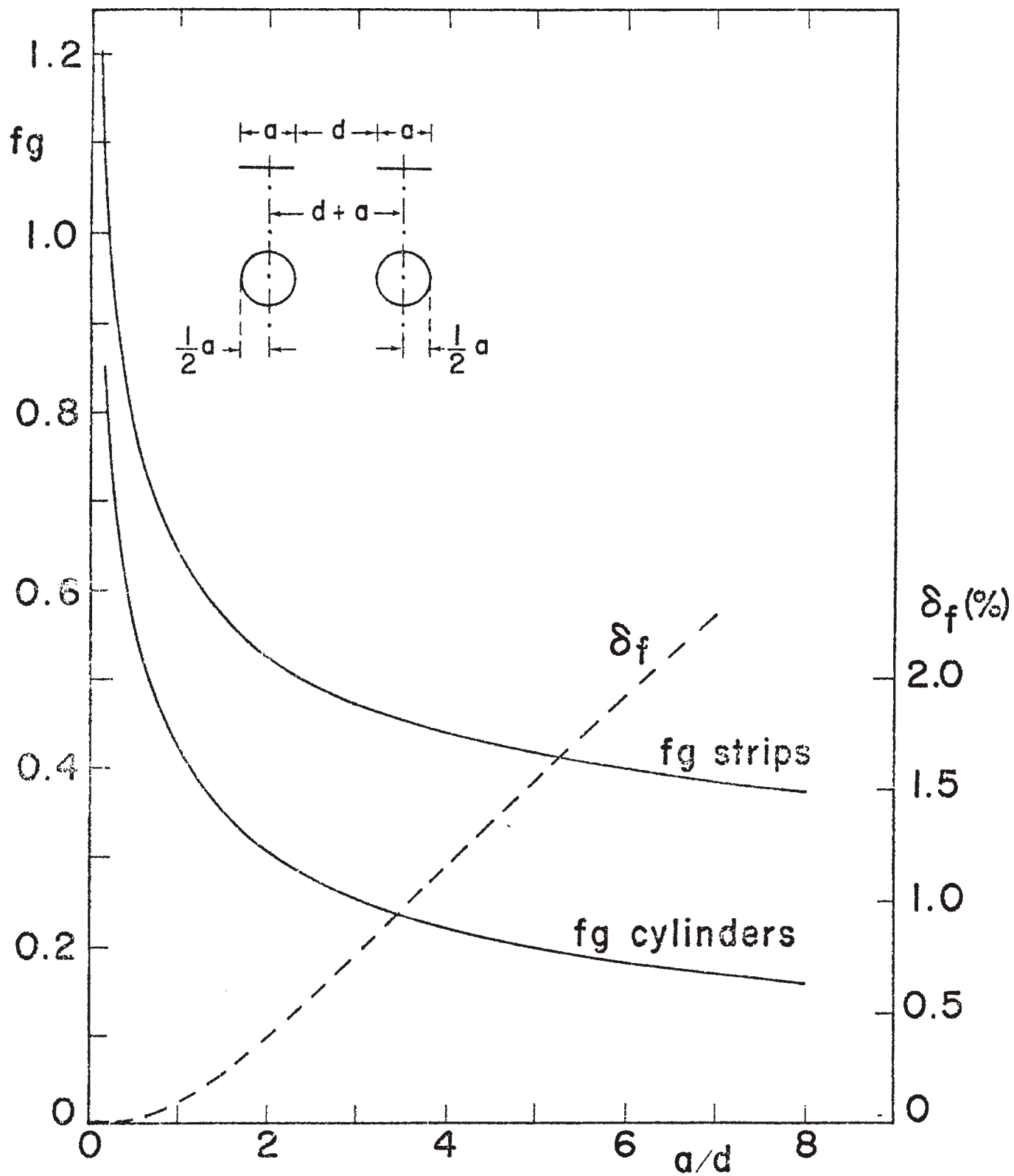


Fig.19. The geometrical impedance factor of a strip transmission line of equal strip width and of a two-cylinder transmission line with radii equal to one half of the strip width. The percentage deviation of the difference of the two factors from  $(\ln 2)/\pi$  is shown as the dashed line.

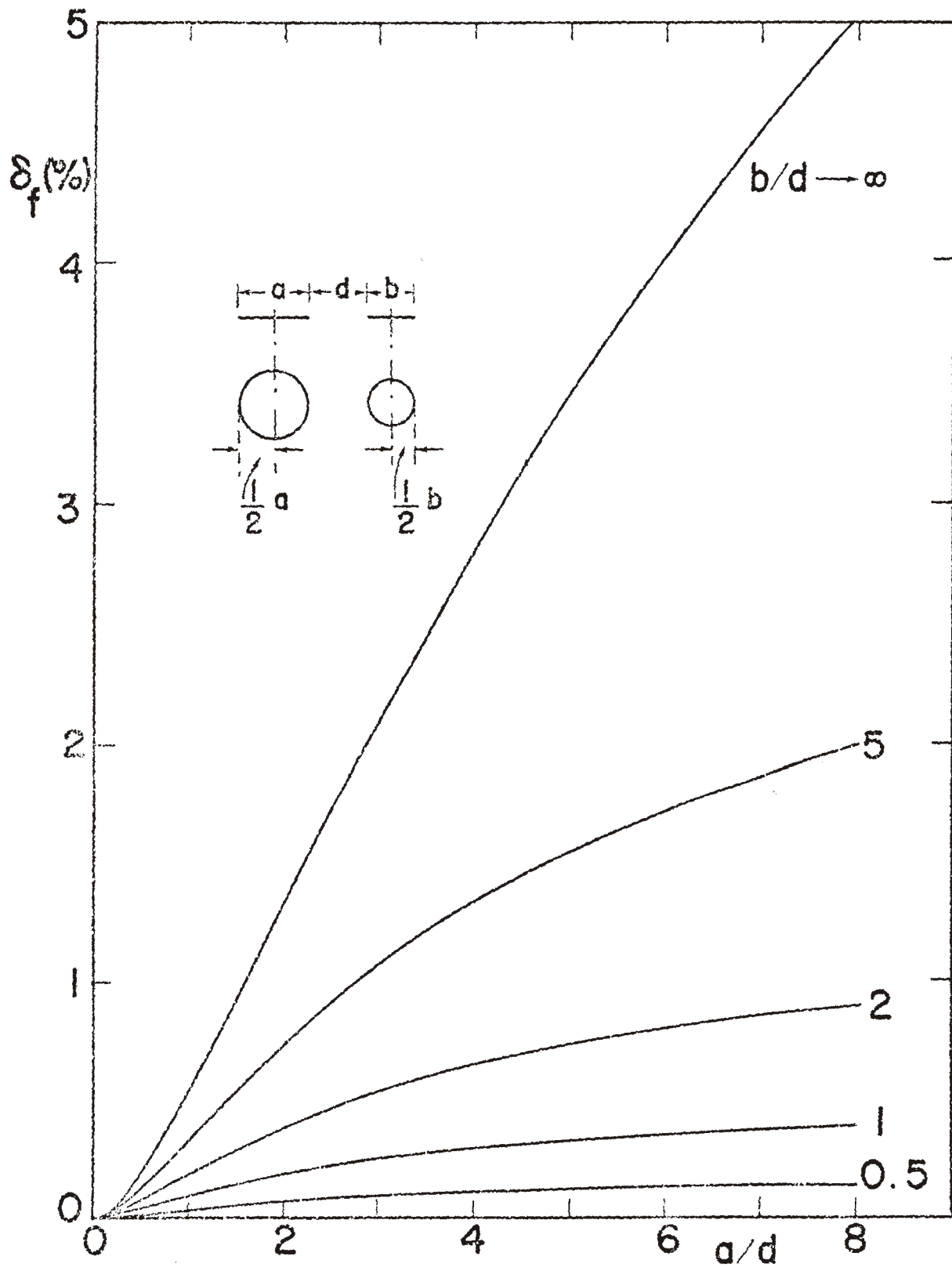


Fig. 20. The percentage deviation of the difference of the two geometrical impedance factors (of the strip line and the two-cylinder line with radii being equal to one half of the strip widths) from  $(\ln 2)/\pi$ .

#### IV. Other Configurations Related to That of the Present Problem

There are many useful configurations that are related to the two coplanar strips of arbitrary widths by simple transformations. We briefly describe these problems in this section.

A logarithmic transformation of the two coplanar strips shown in Fig. 21a results in an infinite stack of parallel strips. One section of the stack is shown in Fig. 21b, where the solid lines denote conductors and the dashed lines denote field lines. In the case that  $V_1 = -V_2 = V$  and the two strips are of the same width, one can introduce infinite conducting planes between the center strip and the outer strips. This is shown in Fig. 21c where the dotted lines denote the images. Hayt [5] showed that the coplanar strips problem is also related to the conventional strip line of Fig. 21d. It has to be noticed that Fig. 21b and Fig. 21d deal with different problems; the latter is for an ordinary strip line.

As pointed out by Baum [10], the coplanar strips case is useful in the study of planar bicone transmission lines (or antennas) --- the use of stereographic projection transforms the planar bicone into two coplanar strips. When the two cones have different cone angles, the stereographic projection results in two coplanar strips of unequal widths. This is shown in Fig. 22.

The use of inversion [8] indicates that the following problems are related to the two coplanar strips case: a strip inside a cylinder (Fig. 23a), a cylinder inside a slit (Fig. 23b), and a strip inside a slit (Fig. 23c).



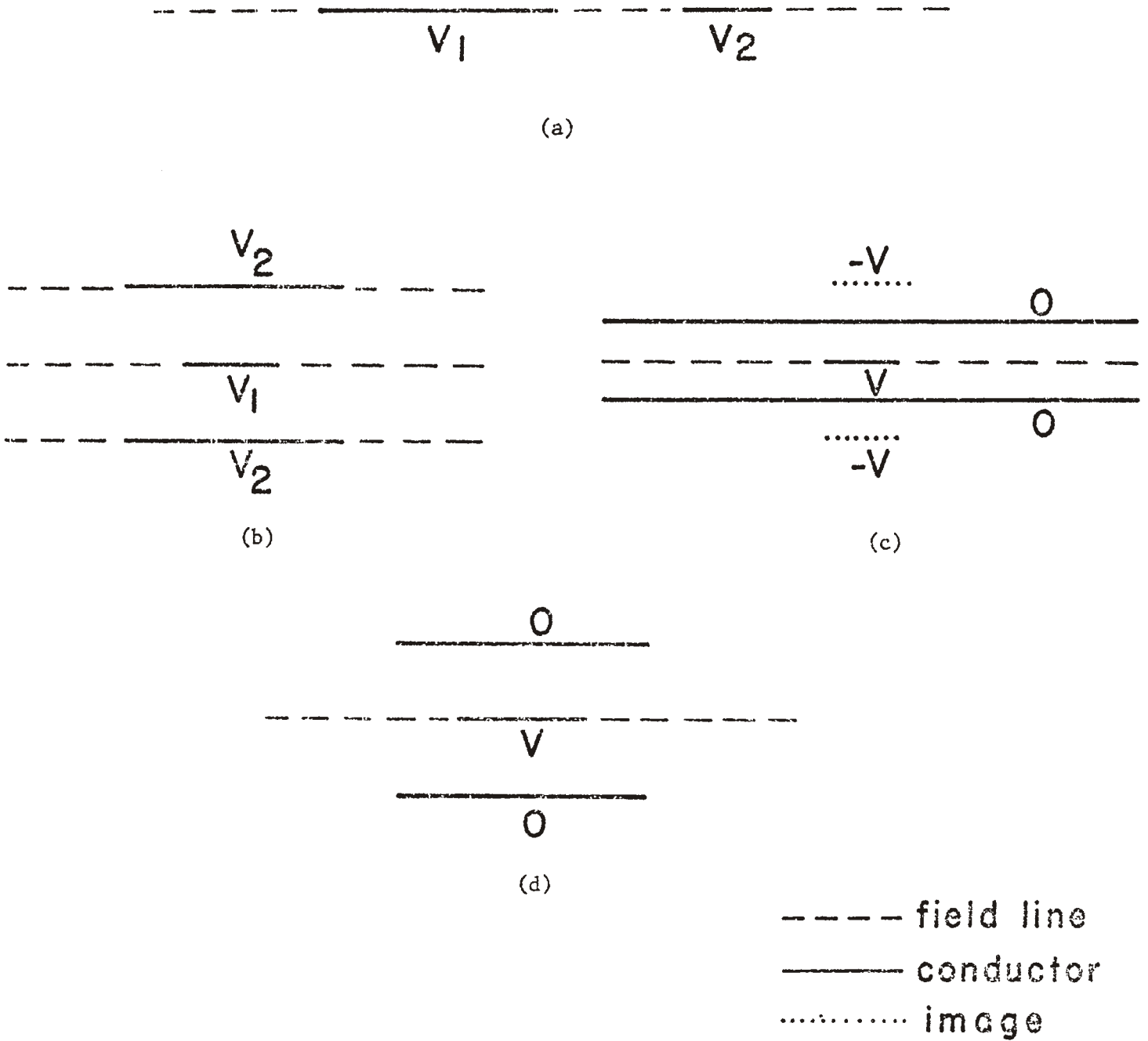


Fig.21. (a) The coplanar strips configuration and its related configuration such as  
 (b) one section of an infinite stack of parallel strips,  
 (c) a strip between two infinite ground planes and  
 (d) the conventional strip line.

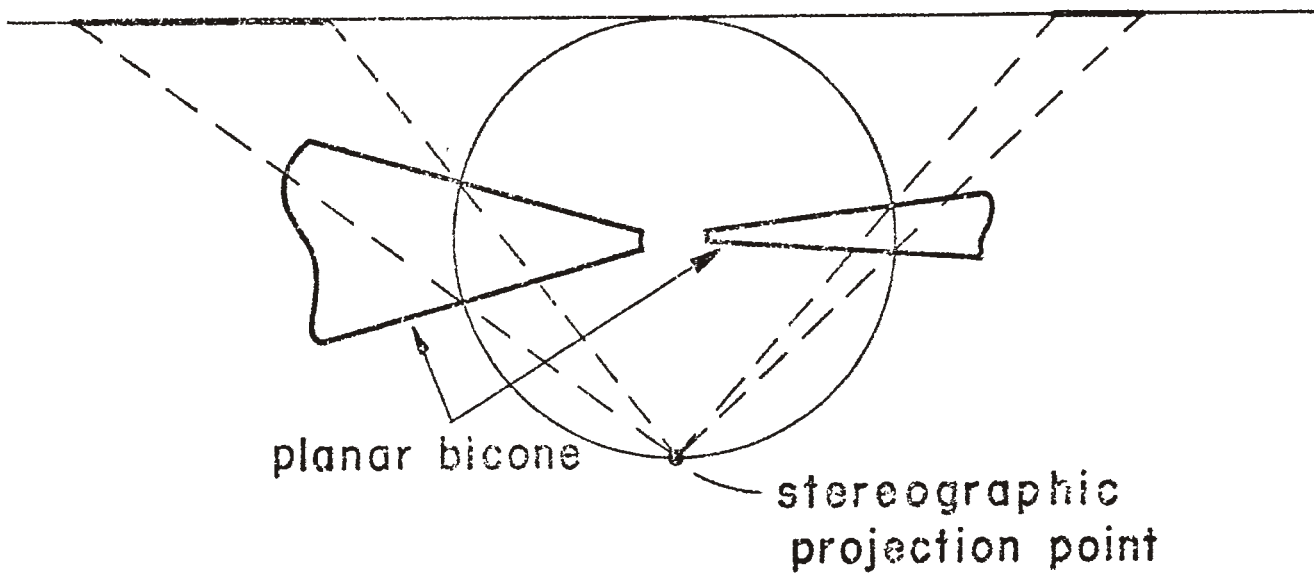
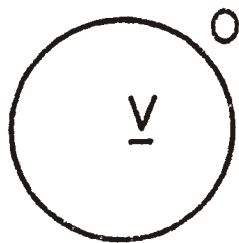


Fig.22. The biconical transmission line and its stereographic projection - the coplanar strips.



(a)



(b)



(c)

Fig.23. Problems related to the coplanar strips by inversion  
 (a) a strip inside a cylinder  
 (b) a cylinder inside a slit  
 (c) a strip inside a slot.

## V. Conclusions

The TEM properties of two unequal widths coplanar strips are obtained by means of successive conformal mapping method. The geometrical impedance factor of such a structure is tabulated, and the field distributions for various cases are presented. The coplanar strips are compared to two parallel circular cylinders. It is found that if the separations between the centers for the two cases are the same and the cylinders have diameters equal to the strip widths, the two geometrical impedance factors differ approximately by a constant  $(1/\pi)\ln 2$ . This relationship is true over a wide range of strip width, and is useful because the two-cylinder formula is more readily available in literature, and is also easier to calculate.

We also point out the various possible extensions of the present work in section IV.

### Acknowledgement

The author wishes to thank Dr. Carl E. Baum, Dr. Kelvin S.H. Lee, and Dr. Lennart O.O. Marin for their numerous suggestions. The manuscript was typed by Mrs. Georgene Peralta and the drawings are prepared by Ms. Theresa Abramian.

## References

- [1] T.K. Liu, K.S.H. Lee and L.O. Marin, "B559 & B561 glide slope track antenna on AABNCP," *DAA Memo 5*, December 1973.
- [2] T.K. Liu, K.S.H. Lee and L.O. Marin, "HF antenna on B-1," *DAA Memo 10*, May 1974.
- [3] C.E. Baum, "Impedances and field distributions for parallel plate transmission-line simulators," *Sensor and Simulation Note 21*, June 1966.
- [4] G.W. Carlisle, "Impedances and fields of two parallel-plates of unequal breaths," *Sensor and Simulation Note 90*, July 1969.
- [5] W.H. Hayt, Jr., "Potential solution of a homogeneous strip line of finite width," *IEEE Trans. on Microwave Theory and Techniques*, vol. MTT-3, pp. 16-18, July 1955.
- [6] P. Moon and D.E. Spencer, *Field Theory Handbook*, Springer-Verlag, 1961. Transformation No. J1.
- [7] M. Abramowitz and I.A. Stegun, *Handbook of Mathematical Functions*, National Bureau of Standards, Applied Mathematics Series 55, 1970.
- [8] W.R. Smythe, *Static and Dynamic Electricity*, 3rd ed., McGraw-Hill, 1968, ch. 4.
- [9] J.D. Kraus, *Antennas*, McGraw-Hill 1950, p. 238.
- [10] C.E. Baum, "Early time performance at large distances of periodic planar arrays of planar bicones with sources triggered in a plane-wave sequence," *Sensor and Simulation Note 184*, August 1973.
- [11] T. K. Liu, K. S. H. Lee and L. O. Marin, "S65-8262-2 VHF communication antenna no.1 on AABNCP," *DAA Memo 14*, July 1973.